Molecularly Imprinted Polymers for Emergency ^{90}Sr Urine Bioassay

by
Negar Hadaeghi Bahraini

A thesis submitted to the Faculty of Graduate Studies and Research in partial fulfillment of the requirements for the Degree of Master of Science

Department of Chemistry
Carleton University
Ottawa, Ontario

April 2011

Your file Votre référence
ISBN: 978-0-494-81695-0
Our file Notre référence
ISBN: 978-0-494-81695-0

Abstract

The present work was focused on the preparation of polymeric submicron particles from methacrylic acid (MAA) to exploit its negative charge (COO^-). The study was performed on two different molecularly imprinted polymer (MIP) particles. The initial tests were performed on MIP particles template with 17β-estradiol (E2) and impregnated with dicyclohexano-18-crown-6 (DCH18C6). The metal ion binding characteristics of these novel particles were studied systematically using both differential pulse anodic stripping voltammetry (DPASV) and atomic emission spectrometry (AES). Our ultimate goal is to develop efficient particles for solid phase extraction of Sr^{2+} from urine samples in emergency bioassay.

The study was continued by investigating on DCH18C6-MIP particles (326±2 nm diameter), which were template with DCH18C6, using acetone and acetonitrile (1:3 v/v) as the porogen, methacrylic acid (MAA) as the functional monomer, and ethylene glycol dimethacrylate (EGDMA) as the cross-linker. The DCH18C6-MIP particles were impregnated with additional DCH18C6 and treated further with NaOH to attain better binding affinity for Sr^{2+}. The effects of pH, ionic strength and amount of particles were evaluated for optimal extraction of $^{90}Sr^{2+}$ from urine samples, as measured by liquid scintillation analysis (LSA). Precipitation and sorption studies were performed for the removal of ^{90}Y interference. After up to 94% of ^{90}Y were removed by sorption onto TiO_2 powders, DCH18C6-MIP particles were applied for the solid phase extraction of ^{90}Sr remaining in the urine matrix, for final LSA. The results showed up to 98% of ^{90}Sr were bound onto NaOH-treated DCH18C6 incorporated MIP particles.

Co-Authorship

The materials discussed in the following chapters have been accepted for publication in:

Journal of Applied Polymer Science

Health Physics Journal

Acknowledgments

The one and half year of my Master's research studies at Carleton University, have been a rewarding experience for me, surrounded by so many intelligent people who have great enthusiasm both for science and life. I would like to express my appreciation to all those people who directly and indirectly contributed to my graduate studies.

I express my gratitude towards my supervisor, Dr. Edward Lai, for his supervision, expert knowledge and scientific comments, which all have contributed to my growth as a student and researcher.

I wish to thank my co-supervisor Dr. Chunsheng Li, for believing in me and who always kindly provided instructive support, accompanied with his positive insights, enthusiasm, and inspiration. I thank Dr. Baki Sadi for his dedication and valuable research discussions and Raymond Ko for our discussions in radiochemistry. I would also like to thank my committee members for taking time out of their busy schedules to generously be on my committee and for their valuable comments on my dissertation.

I would like to acknowledge my sincere gratefulness to Dr. Robert Burk and Dr. P. Sundarajan, This rewarding experience would not be possible without the opportunity of qualifying year, completion and graduate studies' admission: Thank you for giving me this opportunity.

I thank Marilyn Stock and Chantelle Gravelle for being so helpful, Tony O'Neil and Peter Mosher for always willing to help, Graham Galway for his experience on DPASV instrumentation, Jim Logan for his expertise on PC, Gerry Moodie for LSC instrumentation training, and all Dr. Lai's lab group members, past and present, for providing a convivial work environment.

I like to thank my friends at Carleton-Chemistry department, thank you for your friendship and support.

My family have given me their unconditional love and support. I would like to express my appreciation and love: to my parents, despite international borders, they provided me with their love and support in all aspects, making it possible for me to focus on my research studies and goal. My only brother Ali, who I love a lot and his wife Honey, for being my best friend. My most appreciation goes to my five year old son Ryan, who I love dearly and missed so many times joy of being and playing with him: Thank you for being so patient with me. And last not least, I would like to express my love and appreciation to my husband Zack, who had taught me and walked me through the synthesis and preparation of the molecularly imprinted polymer at the early days of my research studies. I would like to thank him for always believing in me, his love, support, for keeping my strength up and understanding me, without me even having to explain.
I would not be where I am today, without my family.

Table of Contents

List of Tables

List of Schemes

List of Figures

List of Acronyms & Symbols

AIBN	azobisisobutyronitrile
AES	atomic emission spectrometry
β	beta
Bq	Becquerel
CBRNE	chemical, biological, radiological-nuclear, and explosives
CPM or cpm	counts per minute
CRTI	CBRNE, Research and Technology Initiative
DCH18C6	dicyclohexano-18-crown-6
DLS	dynamic light scattering
DDW	deionized water
DPASV	differential-pulse anodic stripping voltammetry
DPS	disintegration per second
DPM	disintegration per minute
E2	17β-estradiol
EDGMA	ethylene glycol dimethacrylate
γ	gamma
LSC	liquid scintillation counting
LSA	liquid scintillation analyzer
MAA	methacrylic acid
MIP	molecularly imprinted polymer
MISPE	molecularly imprinted solid phase extraction
NIP	non-imprinted polymer

RN	radiological-nuclear

CHAPTER I

INTRODUCTION

Introduction

1.0 ^{90}Sr Background and Health Effects

Since the 9/11 attacks, the fear of terrorist groups using dirty bombs (radiological weapon, combined with radioactive material and conventional explosives), has increased significantly. Managing exposure to radiation became a major concern to the government and society. One of the efforts made was the CRTI (chemical, biological, radiological-nuclear, and Explosives (CBRNE) Research and Technology Initiative), which was launched in May 2002 as the federal science community's response to providing solutions to CBRN terrorist threats.[1] The mandate of the CRTI is to fund projects in science and technology that will strengthen Canada's preparedness for, prevention of, and response to potential CBRNE threats to public safety and security.[2]

The present thesis is part of the CRTI06-230RD (Rapid Methods for Emergency Radiobioassay), focusing on the rapid extraction and measurement of ^{90}Sr in urine bioassay.

^{90}Sr is one of the fission by-products of uranium (^{235}U) or plutonium (^{239}Pu) with a large fission yield, which is considered the most dangerous component of radioactive fallout, due to its long half-life (29 years). Since strontium has the same valance shell electron configuration as calcium, it can potentially pose a high health hazard, if ingested or inhaled. ^{90}Sr will substitute for calcium and accumulate in the bones. In large enough amounts, this can increase the risk of leukemia and other cancers. Direct exposure to ^{90}Sr can also be harmful to the body because of the high-energy beta particles. Depending on

the maximum energy, these particles can penetrate a few microns to a few centimeters of tissue.[3]

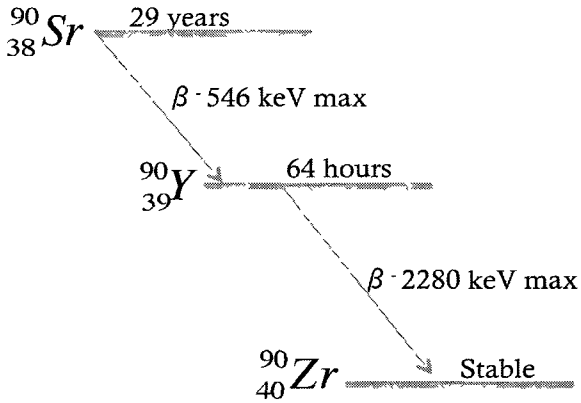

$$^{90}_{38}Sr \rightarrow {}^{90}_{39}Y + \beta^- + \bar{\nu} + E$$

Scheme 1 ^{90}Sr and ^{90}Y decay scheme

Beta particles released by ^{90}Sr (with a maximum energy of 546 keV, 100% intensity) can increase the risk of developing cancer.[4] Therefore a rapid and efficient bioassay method is desired in support of medical response.[9]

Several analytical methods, for determination of ^{90}Sr have been developed in the recent years, such as strontium-specific chromatography with 6-8 h sample turn over time,[9] liquid-liquid extraction and ion-exchange methods, which all tend to be time consuming and labor intensive. Hector et al. (2000) reported the precipitation of yttrium in periodic acid.[5] O'Hara et al. (2009) developed an automated system for the separation

of ^{90}Sr and ^{90}Y in 0.1 M nitric acid, using a strontium-selective sorbent (Superlig 620) obtained from IBC Advanced Technologies (American Fork, Utah, U.S.A.).[6]

Pisarcikova et al. (2007) used dicyclohexano-18-crown-6 (DCH18C6) and picric acid for the extraction of radio-strontium from soil.[7] Plionis et al. (2008) reported an automated procedure for the determination of ^{90}Sr in aqueous sample by flow scintillation analysis. However, they used commercially available Sr-Spec resin, consisting of 4,4'(5')-bis (tert-butylcyclohexano)-18-crown-6 impregnated on polymer beads.[8] Sadi et al. (2010) developed a rapid bioassay method for the measurement of ^{90}Sr in urine for emergency preparedness,[9] which was successfully applied on a field deployable instrument by Li et al. (2009)[10].

It is well known that ^{90}Sr decays to the isotope ^{90}Y, (pure beta-emitter with maximum energy of 2280 keV, 100% intensity). In the presence of interference of ^{90}Y, the LSC is unable to adequately resolve the spectra of these two radionuclides.[11] Therefore, a simple and economic rapid bioassay method, for ^{90}Sr measurements (with minimal interference by yttrium) is still an important topic and requires further scientific investigation.

In the present work, molecularly imprinted polymer (MIP) particles comprising DCH18C6 as a sorbent for rapid and efficient solid phase extraction (SPE) of ^{90}Sr in a urine bioassay is prepared. During molecular imprinting, a cross-linked polymer matrix is formed by free radical copolymerization of functional monomers with an excess of

cross-linkers around the DCH18C6 molecules.[12] The resultant MIP particles are equipped with DCH18C6 sites that bind to Sr^{2+} in urine samples.

This easy and cost-effective method can benefit from the direct suspension of DCH18C6-MIP particles in the liquid scintillation cocktail, for a rapid measurement of $^{90}Sr^{2+}$ uptake in a urine bioassay by LSA.

These particles can be stored dry, without any significant loss of DCH18C6 or lengthy reconditioning, for emergency use.

1.1 Methodologies on ^{90}Sr Emergency Urine Bioassay

During a radiological-nuclear (RN) emergency, first responders and civilians face the danger of contamination by radionuclides through inhalation, ingestion, or wounds.[13] Treatment is possible within the first 48 hours of contamination. Therefore rapid bioassay methods for internal contamination are important for managing the consequences of an RN attack, including the identification of contaminated individuals for early medical intervention.[13] For urinalysis, urine samples must be acidified and processed in a laboratory before quantification is possible. Screening for very high levels of radioactivity can be done in the field and samples should be submitted in well-sealed plastic or glass bottles.

^{90}Sr measurements (β-decay counts) can be done through liquid scintillation analysis. The sample (containing radioisotopes) is dissolved in a cocktail, which contains an

organic aromatic solvent with a high π electron density. β-particles emission will cause solvent molecules to become excited and produce fluorescence. Because the photo multiplier tubes are not sensitive to the fluorescence wavelength of the aromatic solvent, a fluor is used in the cocktail to capture the solvent fluorescence energy and produce photons of light at a detectable wavelength.[14] The intensity of scintillation light is proportional to the initial energy of each beta particle. By placing a vial containing a radionuclide and scintillation cocktail into a dark enclosure, a counter (or detector) can measure the photon intensity. The amplified signal is converted to an electrical pulse, which is registered as one count. Any factor that reduces the efficiency of the β energy transfer or causes the absorption of photons, results in quenching.[15]

In LSA, quenchers are customarily divided into the categories of chemical quenchers and color quenchers. Chemical quenchers absorb radioactive energy before it is converted to light. Therefore, chemical quenchers reduce the number of photons generated by each β-particle. Color quenchers absorb light in the range of the wavelength emitted by the scintillator. In this case the number of photons emitted is not changed, but the number reaching the photomultiplier tube is reduced.[16] Quenching manifests itself by shifting the energy spectrum toward lower energy channels in the multichannel analyzer.[17] If the quench varies from sample to sample, a correction factor should be applied.

One of the methods for quench correction is to manually set the counting window (on the PC monitor connected to LSC) to the desired settings. The other method for quench correction is to use a radioactive nuclide as internal standard. An unknown

sample is first measured and its CPM value is recorded. A known amount of the internal standard is then added to the cocktail and the sample is recounted.

The counting efficiency is defined as:[18]

$$\text{Eff} = \frac{\text{CPM (sd + x)} - \text{CPM (x)}}{\text{DPM (sd)}}$$

The DPM value of the unknown sample can be now calculated:

$$\text{DPM(x)} = \frac{\text{CPM (x)}}{\text{Eff}}$$

Where:

Eff = counting efficiency

CPM(x) = recorded CPM value of sample

CPM(sd+x) = recorded CPM value of sample spiked with internal standard

DPM(sd) = activity of internal standard

^{90}Sr and its daughter ^{90}Y are both beta emitters. The spectra produced by beta emissions from these two nuclides overlap significantly in the liquid scintillation counter. Therefore the interference of ^{90}Y needs to be removed, either chemically or physically. The determination of ^{90}Sr by β-counting requires that ^{90}Sr be separated from ^{90}Y and other interfering radionuclides in the sample matrix.[19]

1.1.1. Solid Phase Extraction for ^{90}Sr / ^{90}Y Separation

As one of the extraction techniques, liquid-liquid extraction has played a major role in sample cleanup. However liquid extraction tends to use large amounts of organic solvents, be labor-intensive and be slow. To overcome the limitations of liquid-liquid extraction, solid-phase extraction (SPE) techniques must be developed.[20] SPE is a separation process by which dissolved or suspended compounds (in a liquid mixture) are separated from each other based on their physical and chemical properties. In SPE, solutes are extracted from a liquid phase into a solid phase.[21] Low cost, ease of automation, highly purified extracts and reduction of organic solvent consumption are few advantages of SPE. A new approach towards developing more specific and selective stationary phases for SPE is molecularly imprinted polymer (MIP).[Error! Bookmark not defined.]

1.1.2. Molecularly Imprinted Solid Phase Extraction (MISPE)

Solid phase extraction (SPE) based on molecularly imprinted polymers (MIPs) is a novel approach for sample preparation and pre-concentration. Molecular imprinted polymers are cross-linked polymer, which contain binding site equipped with functional groups[21,] designed to bind one target compound or a class of structurally related compounds with high selectivity. MIP's are highly stable and can withstand heating to temperatures higher than 120 °C and treatment with organic solvents, strong acids and bases with only small losses in selectivity.[22,23]

These molecularly imprinted polymers can be produced in a covalent or a non-covalent manner. Covalent interaction provides more homogeneous binding sites. The

rebinding is slow because covalent bonds between the template and the MIP have to be formed. Unfortunately, only a limited number of compounds can be imprinted by this approach. In covalent imprinting, the template is chemically coupled with one of the building blocks of the polymer, and, after the polymerization, the resulting bond must be cleaved to obtain free selective binding sites.[23]

Non-covalent imprinting, which relies upon self-assembly between the template and functional monomers, based on hydrogen bonding, Van der Waals forces, electrostatic or hydrophobic interactions, seems more versatile, easier than the former and it is the most employed for preparing SPE phases.[24, 25] In non-covalent imprinting, the binding energies are weak compared to a covalent band. However when weak interactions are present as multiple docking points, they lead to strong binding between two entities.[20]

Choosing a functional monomer complement to the template, is an important step in non-covalent imprinting as the process is relied on the self-assembly of template and functional monomer. Normally for templates with acidic groups, basic functional monomers are chosen, carboxylic acids and amides high selectivity have observed with acrylamide and methacrlamide.[26] The more interaction between the template and functional monomer, the better the binding and selectivity.

MIP Non-covalent synthetic approach typically involves free radical polymerization of functional vinyl monomers with an excess of divinyl cross-linking

monomers in the presence of a molecular template, which controls the distribution of functional groups in the resulting three-dimensional polymer network. After polymerization and template removal, specific binding sites are left in the polymer material, which can be used to afford effective selective separation.[27] Functional monomers are responsible for the binding interactions in the imprinted binding sites and, for non-covalent molecular imprinting protocols, are normally used in excess relative to the number of moles of template to favor the formation of template, functional monomer assemblies. It is clearly very important to match the functionality of the template with the functionality of the functional monomer in a complementary fashion. Hydrogen bond is most often applied as a molecular recognition interaction of molecularly imprinted polymers. From this, acrylic acid and methacrylic acid have usually been adopted as functional monomers, since carboxyl group functions as a hydrogen donor and a hydrogen acceptor at the same time.[28]

Acrylic Acid 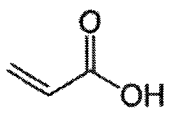

Methacrylic Acid 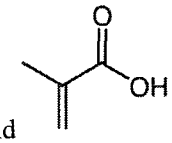

Although moving to higher functional monomer to template ratios, follow the Le Chatelier principle favoring the equilibrium toward an increase in polymerization and complex formation, it also leads to increased levels of non-specific binding.[28] Lower functional monomer-template ratios will lead to lower site population densities in the polymer. The geometry of the imprinted sites and the correct positioning of the functional groups will be retained in a rigid polymer network. Therefore a high amount of cross-linker compared to the amount of template-monomer is required.

Template, functional monomer, cross-linker and initiator should be able to dissolve in mixture porogenic solvents. Porogenic solvents play an important role in formation of the porous structure of MIP. It is known that the nature and level of porogenic solvents determines the strength of non-covalent interactions and influences polymer morphology, which obviously, directly affects the performance of MIP. The porogenic solvents should be relatively low polarity, in order to reduce the interferences during complex formation between the imprint molecule and the monomer, as the latter is very important to obtain high selectivity MIP.[28] In another paper, Yu et al. (2010) specified, when the porogen had poor hydrogen bonding, the interaction energy was mainly influenced by the dielectric constant of the solvent. When the porogen had a strong capacity in forming the hydrogen bond, both the dielectric constant and the hydrogen bonding would affect the formation of the template–monomer complex. This computational study strongly suggested that the interaction energy between the template and monomer varied with the pre-polymerization solution composition.

When using aprotic solvents (such as chloroform, toluene and acetonitrile), the interaction energies are mainly influenced by their dielectric constants. The smaller the dielectric constant is, the stronger the complexation between template and monomer will be. When using solvents (such as methanol) with a high capacity to form hydrogen bonds, the hydrogen bonding would affect the formation of the template-monomer complex, thus influencing the interaction energy.[29]

1.1.3. Incorporating Crown Ethers

Separation and extraction of the actinides by complexation with crown ethers is one of the many proposed methods. Crown ethers, first introduced by Pederson in 1967, are synthetic macro-cyclic polyethers consisting of essential ethyleneoxy (-CH_2CH_2O-) repeating units, which have a cavity of specific size. The oxygen atoms inside the cavity, can act as a Lewis bases due to the presence of lone pairs and electron donor ligand atoms.[30] Tailor-making metal-specific ligands by attaching them to polymeric carriers is an excellent way of meeting the increasing demand for materials suitable for the separation of metal ions from complex sources.[31]

In recent years, highly selective extraction chromatographic materials have been developed in which macrocycles are covalently attached or sorbed[32] onto solid supports. The complexation behavior of alkali and alkaline earth elements can best be described in terms of "host-guest complexation" which requires complementary size matching of ionic radii and ligand cavities. This suggests that crown ethers and ions that match in size would form stable complexes.

The stability of the complexes formed also depends on the nature of the electron donor atoms present in the ligand and metal ions in aqueous phase. Based on the hard and soft acids and bases (HSAB) theory, the hard and soft cations are stably complexed by hard and soft electron donors respectively.[60]

Earlier studies showed that Sr^{2+} metal ion (ionic radius 132 pm) is completely

encapsulated in the cavity of 18-Crown-6 (cavity radius 130-160 pm) due to its appropriate size matching within the cavity.[33] On the other hand crown ether ligand with oxygen as donor atom acts as a hard base, therefore based on the HSAB principle crown ether prefers to hard metal ions such as Sr^{2+}.

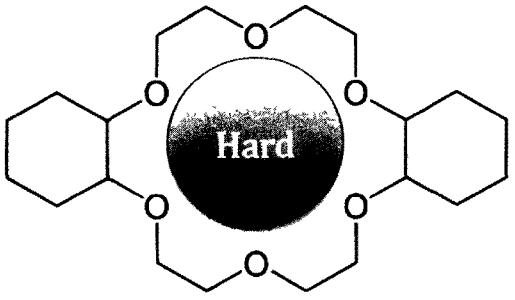

Figure 1 Dicyclohexano-18-crown-6 (DCH18C6). The hard base cavity prefers to bind with hard cations.

The selective complexing properties exhibited by crown ethers towards metal ions have led to their incorporation into polymeric matrices[31] and potentially useful in conjunction with molecular imprinting.[34]

1.1.4 ^{85}Sr as a surrogate for ^{90}Sr

^{85}Sr can be employed as a surrogate in place of ^{90}Sr, to take advantage of its easy measurement by gamma spectroscopy without interference by ^{90}Y. Gamma photons have no mass and no electrical charge; they are purely electromagnetic energy. In γ decay, electromagnetic radiation is produced as a nucleus undergoes transition from its higher excited state to a lower excited state or its ground state.[35]

$$ {}^{A}_{Z}E^{*} \rightarrow {}^{A}_{Z}E + \gamma $$

Gamma spectrometers are each equipped with a detector appropriate for measuring the photon energy. There are several types of gamma spectrometers designed for different applications. The most common type is the inorganic scintillators, mostly equipped with a NaI (Tl) detector.[36] The NaI crystal is doped with thallium (Tl) as activation impurities for counting gamma rays with a linear energy response.[65] In a scintillator, interaction of photons with the crystal results in the excitation of atoms to higher energy states, followed by their immediate relaxation with consequent emission of light photons.[36] A radiation detector can identify the energy of the incoming gamma ray by counting the photons generated.

1.1.5. The SI unit of radioactivity

The becquerel (symbol Bq) is the SI unit of radioactivity. 1 Bq is defined as the activity of a quantity of radioactive material in which one nucleus decays (or disintegrates) every second. When the radioactivity of a sample is measured with a detector, the unit of "counts per second" (cps) or "counts per minute" (cpm) is often used. These units can be converted to the absolute activity in Bq.[37]

1 Becquerel (Bq) = 1 disintegration per second

1dpm = 60 dps (Bq)

Counts per minute (cpm) = cpm measured in sample - background cpm

Efficiency = cpm / dpm (disintegration per minute)

Activity = cpm / efficiency

Equivalent dose of radiation is called sieverts (symbol Sv); sievert is a unit that takes account of the effects of different types of radiation on the human body.

$1\ Sv = 1\ J\ kg^{-1}$

The rate of decay is called activity (A). The activity represents the number of parent nuclides that decay per unit time.[42]

A = A(0) × exp((-0.693/half-life in days) × t

For the conversion of activity (Bq) to concentration (Pico meter):

$$L = \frac{Ln2}{H}$$

$$N = \frac{A}{L}$$

$$N = \frac{grams\ \ of\ \ element}{Atomic\ \ mass} \times (6.02 \times 10^{23})$$

Where N is the number of atoms, A is activity (Bq) and L is decay constant per second which H is half-life of isotope in seconds. Once the atom quantity has been determined, conversion to mass (or mass concentration) is the same as for all other elemental calculations.[43]

1.2 Aim of This Study

The principle objective of this research is to develop an emergency response technique for the determination of ^{90}Sr in urine samples. For this propose:

- Development of a molecularly imprinted polymer (MIP) comprising dicyclohexano-18-crown-6 (DCH18C6) as a sorbent is evaluated for optimal extraction of $^{90}Sr^{2+}$ from urine samples, as measured by liquid scintillation analysis (LSA).

- Removal of ^{90}Y interference prior to ^{90}Sr measurement.

- Development of a NaOH treated DCH18C6-MIP particles for the best possible ^{90}Sr extraction in a range of urine pH and ionic strength (due to individual diet).

- Direct suspension of MIP particles bound to ^{90}Sr in the liquid scintillation cocktail for convenient measurement.

CHAPTER II

EXPERIMENTAL

2.0. Materials

17β-Estradiol (E2), methacrylic acid (MAA), ethylene glycol dimethacrylate (EGDMA), 2,2′-azobis(2-isobutyronitrile) (AIBN), dicyclohexano-18-crown-6 (DCH18C6), periodic acid (H_5IO_6), potassium iodate (KIO_3), Nitrate salts of Cd^{2+}, Pb^{2+} and Cu^{2+} were all purchased from Sigma-Aldrich (St. Louis, MO, U.S.). Titanium dioxide (TiO_2) powders were purchased from Anachemia. Acetonitrile (HPLC grade) and acetone were of analytical-reagent grade, as obtained from Caledon (Georgetown, ON, Canada). Optiphase Hisafe 3 liquid scintillation cocktail was purchased from PerkinElmer (Woodbridge, ON, Canada); Wheaton glass scintillation vials (20 mL) were purchased from Fisher Scientific (Ottawa, ON, Canada). ^{85}Sr standard and ^{90}Sr standard were obtained from Eckert Ziegler (Valencia, CA). ^{85}Sr was 1000 Bq mL^{-1} in 3 M HNO_3 with 50 μg mL^{-1} stable strontium as carrier. ^{90}Sr was 372 Bq mL^{-1} in 0.1 M HCl with 100 μg mL^{-1} stable strontium and 10 μg mL^{-1} stable yttrium as carriers. Urine samples were stabilized by acidifying to 1 % (v/v) HCl, and stored at 4-8°C until use.

2.1. Investigation on MIP binding characteristics

The metal ion binding characteristics of molecularly imprinted polymer (MIP) submicron particles prepared using 17β-estradiol (E2) as a template, and incorporated with dicyclohexano-18-crown-6 (DCH18C6), were studied using differential pulse anodic stripping voltammetry. When Sr^{2+} was added to DH18C6-E2-MIP particles already occupied by Cd^{2+}, Cu^{2+} and Pb^{2+} inside the binding sites, a displacement reaction was observed.

This demonstrated that DCH18C6 had stronger binding affinity for Sr^{2+} than Cd^{2+} Cu^{2+} or Pb^{2+}. Strong DCH18C6 binding affinity was also observed for Y^{3+}. Atomic emission spectrometry showed that DCH18C6-E2-MIP particles (150 mg/mL) resulted in 52% binding of Sr^{2+} (2000 ppm, at pH 6.3±0.1 and ionic strength of 0.1 M $NaNO_2$).

2.1.1. Preparation of molecularly imprinted polymer particles

The method for synthesizing E2 and DCH18C6, MIP particles was adopted from a previous report by Lai et al. (2010). [4] A molar ratio of 1:8:4 was used, by dissolving E2 (0.272 g) or DCH18C6 as the template, MAA (0.343 mL) as the functional monomer, EGDMA (0.668 mL) as the cross-linker, and AIBN (0.0234 g) as the initiator in 40 mL acetone/acetonitrile (1:3 v/v) as the porogen. The mixture was deoxygenated with nitrogen for 5 min, and then polymerized at 60°C for 24 h in a water bath. The E2-MIP particles were then washed 3 times with acetonitrile to remove any remaining chemicals, collected by centrifugation, and dried at 70°C in an oven. The average particle size was measured by dynamic light scattering (DLS) using a nanoDLS analyzer (Brookhaven Instruments, Holtsville, NY, U.S.).

2.1.2. DCH18C6 as binding ligands in E2-MIP particles

Different concentrations (86-500 ppm) of DCH18C6 were added, in 5-mL aliquots, to 75 mg of E2-MIP particles in each microtube. After incubation for 1 hour, the microtubes were centrifuged at 3400 ±100 rpm for 50 min. The supernatant was withdrawn for high performance liquid chromatography (HPLC) analysis with UV detection to determine the remaining DCH18C6 concentration, and hence the quantity of

DCH18C6 incorporated by the E2-MIP particles. The DCH18C6-E2-MIP particles were washed, collected and dried for binding tests. 75 mg of DCH18C6-E2-MIP particles were added into 0.5 mL of standard metal solution (containing 10^{-5} M of Cd^{2+}, Cu^{2+}, Pb^{2+}, Sr^{2+} and/or Y^{3+}). After incubation for 1 hour, the mixture was centrifuged for 50 min to collect all particles on the bottom. Upon transferring 0.1 mL of the supernatant into a voltammetric cell containing 10.5 mL of supporting electrolyte solution, DPASV analysis was performed to determine the remaining Cd^{2+}, Cu^{2+} and Pb^{2+} concentrations.

2.1.3 HPLC analysis and DPASV analysis

HPLC analysis was performed on a Perkin Elmer LC240 instrument. The mobile phase was composed of acetonitrile/methanol/distilled deionized water (1:1:2 v/v) at a flow rate of 0.5 mL/min, and the UV detector was set at a wavelength of 278 nm.

DPASV was used to determine the binding efficiency of E2-MIP and DCH18C6-E2-MIP particles with trace concentrations of Cd^{2+}, Cu^{2+} and Pb^{2+} at room temperature. All analyses were performed on a Metrohm model 797 VA instrument, with an Ag/AgCl reference electrode and a hanging mercury drop working electrode. 10.5 mL of supporting electrolyte solution (containing 0.5 mL of 0.1 M acetate buffer), 0.1 mL of 3 M KCl, and 0.1 mL of supernatant were added in the voltammetric cell. The solution was deoxygenated with high-purity nitrogen, and then analyzed by setting the initial potential to -1.2 V, the final potential to -0.1 V, the deposition time to 60 s, the step potential to 2 mV, and the frequency to 50 Hz. Determination of Cd^{2+}, Cu^{2+} and Pb^{2+} concentrations was achieved by the standard addition method. Data acquisition and analysis were controlled through a PC computer connected to the potentiostat.

2.2. Radio-strontium binding studies

For the initial investigation, ^{85}Sr was employed as a surrogate in place of ^{90}Sr, to take advantage on easy gamma spectrometric measurements on a Triathler Multilabel 425-004 Tester (Hidex Oy, Finland) without any interference of ^{90}Y. Experiments were conducted in DDW then continued in urine metrics.

2.2.1 Preparation of molecularly imprinted polymer particles

The method for synthesizing DCH18C6-MIP particles was similar for E2-MIP particles, described earlier.[7] Scheme 2 summarizes this method for DCH18C6-MIP particles.

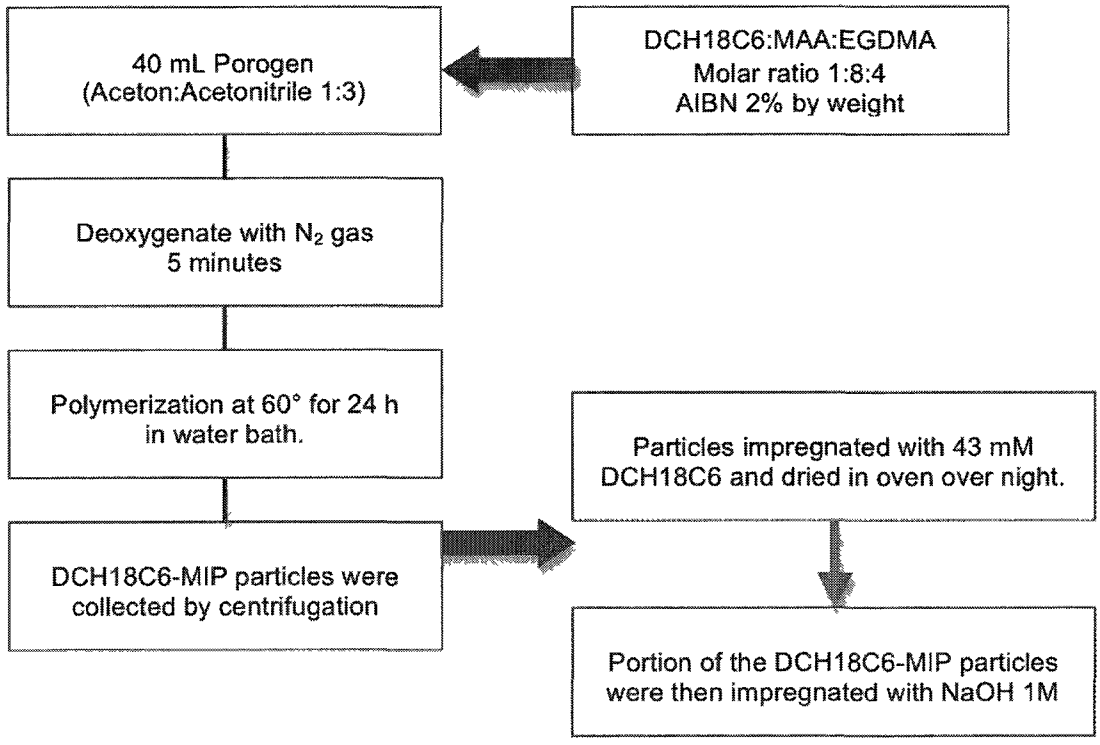

Scheme 2 Summary of DCH18C6-MIP particles synthesis.

Each 500 mg of impregnated DCH18C6-MIP particles, as shown in Scheme 1 were then treated with 1 mL of NaOH (1 M), sonicated for 1 h, and dried (for further improvement with respect to Sr uptake). The average particle size for DCH18C6-MIP particles was measured to be 326±2 nm, by dynamic light scattering (NanoDLS, Brookhaven Instruments, Holtsville, NY, U.S.).

2.2.2. Determination of strontium uptake

For the initial study in this part binding of Sr^{2+} onto DCH18C6-E2-MIP particles was studied further by atomic emission spectrometry (AES) at 407.7 nm or 421.5 nm. Various concentrations of stable strontium (400, 800 and 1600 ppm) in DDW (pH adjusted to 4.1 by NaOH 5M) were added to 150 mg E2-MIP particles which were incubated with DCH18C6 11 mM. After one hour sonication, the supernatant was separated by 50 minutes of centrifugation and transferred for atomic emission spectrometry at 421.5 nm.

To determine strontium uptake by MIP particles incorporated with DCH18C6, ^{85}Sr was employed to take advantage of easy gamma spectrometric measurements on a Triathler Multilabel 425-004 Tester (Hidex Oy, Finland). The uptake was investigated as a function of pH, ionic strength and amount of particles, using a stock solution that contained 1000 Bq mL^{-1} ^{85}Sr in 3 M HNO_3 together with 50 μg mL^{-1} stable strontium as carrier. Due to the decay of ^{85}Sr (half-life of 65 days), its actual amount was not the same for all uptake experiments.

For the study of pH and ionic strength effect, aqueous solutions containing 100 Bq $^{85}Sr^{2+}$ were pre-conditioned by NaOH (5 mol L^{-1}) to various pHs (1.0, 5.5, 6.3). Samples were preconditioned once two different concentrations (0.1 & 1 M) of $NaNO_2$. For each solution, aliquot of 3 mL was added to 150 mg of MIP particles incorporated with 11 mM DCH18C6. After 80 min of sonication, the solid phase was separated by 50 minutes of centrifugation at 4000 rpm. 0.5 mL aliquot of the supernatant was transferred to a vial for the determination of the remaining $^{85}Sr^{2+}$ concentration by gamma spectroscopy.

The effect of DCH18C6 concentration onto ^{85}Sr uptake was investigated. E2-MIP particles were incubated with different concentrations of DCH18C6 (11, 22, 43 and 54 mM). 100 Bq $^{85}Sr^{2+}$ were pre-conditioned with $NaNO_2$ 0.1M and pH was adjusted by NaOH (5 mol L^{-1}) to 6.3. After 80 min of sonication, the solid phase was separated by 50 minutes of centrifugation at 4000 rpm. 0.5 mL aliquot of the supernatant was transferred to a vial for the determination of the remaining $^{85}Sr^{2+}$ concentration by gamma spectroscopy. DCH18C6-E2-MIP and DCH18C6-MIP (both incubated with 43 mM DCH18C6) were compared, following the same method described above.

The pH effect was further investigated for the binding studies of ^{90}Sr and ^{90}Y onto DCH18C6-MIP particles, in various pHs (2.5, 5.5, 6.3, 6.5, 7.5, 8.5 and 9), urine samples (3 mL), each being spiked with 100 Bq $^{90}Sr^{2+}$ and $^{90}Y^{3+}$. After separation of the solid phase by centrifugation, 0.5 mL aliquot of the supernatant was diluted with 4.5 mL of DDW (to be comparable with those standard solutions in the calibration cassette for Tri-Carb liquid scintillation) and then mixed with 15 mL of Optiphase Hisafe 3 liquid

scintillation cocktail. The uptakes of $^{90}Sr^{2+}$ and $^{90}Y^{3+}$ by DCH18C6-MIP particles, at an optimal pH of 6.3-6.8, were measured by a Tri-Carb 3180/SL liquid scintillation analyzer (LSA) (Perkin Elmer, Woodridge, Ontario, Canada) for a one-hour read of each sample. The same pH effect was further investigated for the ^{90}Sr and ^{90}Y uptake onto NaOH treated DCH18C6-MIP particles in the pH range 0.82 – 7.24.

To study the effect of ionic strength on strontium uptake by DCH18C6-MIP particles, experiments were conducted in the presence of various sodium salts that consisted of anions from the Hofmeister series ($NaNO_2$, $NaNO_3$ or NaI) both in DDW and urine (Mracek et al. 2008). In particular, ion strengths of 0.1 M and 0.3 M were investigated for 2-mL sample solutions containing 30 Bq $^{85}Sr^{2+}$ (pre-adjusted to pH 6.3 with 5 mol L^{-1} NaOH) and 150 mg of particles. After sonication for 1.5 h and centrifugation, the supernatants were measured by gamma spectroscopy to determine the remaining concentration of $^{85}Sr^{2+}$. $NaNO_2$ was found to be the best salt for providing an optimal ionic strength.

To study the effect of the amount of DCH18C6-MIP particles on strontium uptake by DCH18C6-MIP particles, 2-mL urine samples containing 30 Bq $^{85}Sr^{2+}$ (pre-adjusted to pH 6.3 and ionic strength of 0.3 M $NaNO_2$) were mixed with different amounts (150, 300, 400 and 500 mg) of DCH18C6-MIP particles. After sonication for 1.5 h and centrifugation, the supernatants were measured by gamma spectroscopy to determine the remaining concentration of $^{85}Sr^{2+}$. 500 mg of DCH18C6-MIP particles showed the

highest $^{85}Sr^{2}$ uptake. The salt effect was further studied for 500 mg of DCH18C6-MIP particles, using pH 6.3 and ionic strength of 0.3 M.

Moreover, the uptake of $^{90}Sr^{2+}$ and $^{90}Y^{3+}$ onto 500 mg of DCH18C6-MIP particles (pretreated with NaOH) were studied at pH 6.3 using $NaNO_2$ at various ionic strengths from 0.1 to 0.5 mol L^{-1}. Competitive $^{90}Sr^{2+}$ and $^{90}Y^{3+}$ uptake, at pH 6.3 and ionic strength of 0.3 M $NaNO_2$, was last measured by a Tri-Carb 3180/SL LSA.

2.2.3 ^{90}Y removal from urine sample prior to MIP addition by precipitation

As described earlier, liquid scintillation counting for ^{90}Sr measurements, suffers from the interference caused by in-growth spectrum of yttrium. Separation by precipitation is one of the most widely used techniques as a conventional treatment method for the removal of ^{90}Y.

In this section the precipitation of ^{90}Y was studied on urine samples spiked with ^{90}Sr and ^{90}Y mixture, in the presence of H_5IO_6, KIO_3 and TiO_2 separately.
Precipitation study using periodic acid (H_5IO_6) was adapted from a previously developed method by Hector et al. 2000. For this study each 3 ml urine samples were spiked with 100 Bq of ^{90}Sr and ^{90}Y. H_5IO_6 in 1:1 molar ratio with yttrium was added to urine samples. The pH was adjusted by NaOH 5M to 2, 2.6 and 5.6. At pH 5.6 a sudden white precipitation occurred. The samples were sonicated for 30 minutes. The white precipitate was then separated by centrifugating the sample for 10 minutes. Then general procedure for the ^{90}Sr and ^{90}Y determination was applied.

The precipitation study of ^{90}Sr and ^{90}Y was studied in the presence of KIO_3 by pre-conditioning the urine samples with KIO_3 0.5 M in various pHs (2.4, 3.5 and 12.5). For this investigation, 70 Bq of ^{90}Sr and ^{90}Y was spiked to 1 ml urine samples. The sample solution's pH was then adjusted to various pH (2.4, 3.5 and 12.5) by NaOH 5 M. Samples were then pre-conditioned with KIO_3 0.5 M until the precipitation occurred. After 30 minutes sonications, the precipitant was separated, by centrifuging the samples for 10 minutes. 0.5 ml of supernatant and 4.5 ml DDW were transferred to the LSC vials. 15 ml of Optiphase Hisafe 3, liquid scintillation cocktail was added to each vial. The concentration of the remaining ^{90}Sr and ^{90}Y was measured by a Tri-Carb 3180TR/SL LSA (liquid scintillation analyzer).

^{90}Y removal was studied, using TiO_2 as an adsorbing surface. Urine samples (3 mL each) were spiked with 100 Bq $^{90}Sr/^{90}Y$ and pre-conditioned to various pH levels (2.6, 4.6, 6.3, 6.5, 6.8, 8.3 and 9.3) by NaOH (5 mol L^{-1}) at an ionic strength of 0.3 M $NaNO_2$. 0.012 g of TiO_2 was then added to each 3 mL urine samples making TiO_2 0.05 M. After sonication (30 min), the solid was separated from the liquid phase by centrifugation (15 min). 0.5-mL aliquots of the supernatants were each diluted with 4.5 mL of DDW and mixed with 15 mL of Optiphase Hisafe 3 liquid scintillation cocktail. The amounts of ^{90}Sr and ^{90}Y were measured by Tri-Carb 3180TR/SL LSA.

Next, the same above procedure was repeated for the investigation on TiO_2 concentration of 0.01 and 0.05 mol L^{-1} in urine samples, pre-conditioned with $NaNO_2$ to

an ionic strength of 0.3 mol L^{-1} at pH 6.3 and spiked with 100 Bq $^{90}Sr/^{90}Y$. The mixture in this part was first vortexed vigorously for ≈1 min, then sonicated for 30 min.

2.2.4 Direct LSC measurement of ^{90}Sr bound to DCH18C6-MIP particles

0.05 M TiO_2 in 3-mL urine samples (spiked with 100 Bq ^{90}Sr and ^{90}Y) were pre-adjusted to pH 6.3 and ionic strength of 0.3 M $NaNO_2$. After sonication (30 min) and centrifugation (15 min) to settle down TiO_2, 0.5 mL of the supernatant was transferred to a vial for LSA measurements. The remaining supernatant was mixed with 500 mg of DCH18C6-MIP particles.

After sonication (40 min) and centrifugation (40 min), 0.5 mL of supernatant and all of the solid phase were transferred to two separate vials. The content of each vial was topped up to 5 mL by adding DDW, followed by 15 mL of liquid scintillation cocktail (Optiphase Hisafe 3). The amounts of ^{90}Sr and ^{90}Y were measured using a Tri-Carb 3180TR/SL LSA.

CHAPTER III

RESULTS & DISCUSSIONS

3.0 MIP binding studies by DPASV

Competitive binding studies of Sr^{2+} and Y^{3+} on MIP particles (already bound with Pb^{2+}, Cd^{2+} and Cu^{2+}) were first performed by using differential-pulse anodic stripping voltammetry (DPASV) analysis. DPASV is among the most sensitive and convenient analytical methods for the trace analysis of heavy metal ion contaminants, such as lead, cadmium, copper and zinc in trace levels in the range of part-per-million (ppm) or even part-per-billion (ppb) molarity.[38] The technique involves a pre-concentration step which the metal ions (M^{n+}) are reduced to their zero valance state phase into hanging mercury drop electrode (working electrode, cathode) at a potential more negative than the half wave potential of the metal ion. Then the selective oxidation of each metal phase species during an anodic potential sweep.[38] Subsequent oxidation of the metal from the mercury drop serves as both the stripping and detection step. This technique provides symmetrically shaped peaks on the current- voltage plots, which the peak currents are proportional to the concentration of the analyte in the amalgam.[39]

Pre-concentration (deposition): $M^{+n} + Hg + ne \rightarrow M(Hg)$

Stripping : $M(Hg) \rightarrow M^{+n} + Hg + ne$

Due to the very negative reduction potential of Sr^{2+}, it is not possible to determine Sr^{2+} directly in aqueous solution by DPASV technique. Therefore equilibrium binding studies were considered as an indirect method in this work to investigate the binding properties of various MIP particle types.

3.0.1. Binding of Cd^{2+}, Cu^{2+} and Pb^{2+} onto E2-MIP particles

The molecular structures of E2, MAA,[40] EGDMA[41] and DCH18C6[42] are illustrated in Fig. 2. The synthesis of E2-MIP particles was simple, involving a one-step suspension polymerization procedure. Their submicron size (153±1 nm as measured by DLS) facilitated uniform dispersion in water for up to 17 days.[43] Capillary electrophoresis provided an estimation of their negative surface charges from the -COOH group of MAA.[44]

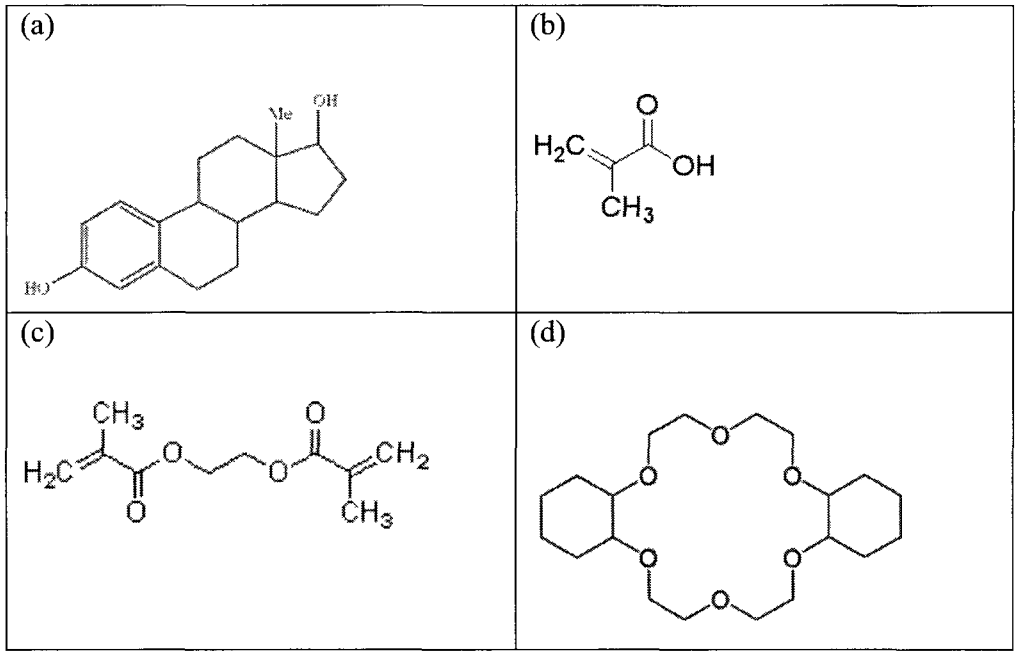

Figure 2 Molecular structures of (a) 17b-estradiol (E2), (b) methacrylic acid (MAA), (c) ethylene glycol dimethacrylate (EGDMA), and (d) dicyclohexano-18-crown-6 (DCH18C6).

Table 1 Ionic radii of metal ions.[45]

Metal	Ionic radius (pm)
Cd^{2+}	109
Cu^{2+}	87
K^{+}	152
Pb^{2+}	133
Sr^{2+}	132
Y^{3+}	104

The DPASV technique lent itself to sensitive determination of small changes in metal ion concentrations, while its low detection limits allowed the use of sample solutions containing as little as 10^{-7} M of metal ions for binding tests. Figure 3(a) shows a DPASV voltammogram that exhibited three characteristic peaks for Cu^{2+} (at -0.11 V), Pb^{2+} (at -0.40 V) and Cd^{2+}(at -0.60 V) simultaneously. The three current peak signals, at each characteristic potential, is related to the concentration of standard added in each step of the standard addition analysis. As shown in Fig. 3(b) to 3(d), up to 84±1% of Cd^{2+}, 90±1% of Pb^{2+} and 90±1% of Cu^{2+} bound with 150 mg of E2-MIP particles in 10.7 mL of aqueous solution. Apparently competitive binding of Cd^{2+}, Pb^{2+} and Cu^{2+} with the E2-MIP particles occurred, and differences in % binding could be attributed to the equilibrium constant between each metal ion and –COOH/-COO- groups from MAA/EGDMA.

A previous study by Kesenci *et al* had used poly(ethylene glycol dimethacrylate-*co*-acrylamide) beads for the separation of Pb^{2+} and Cd^{2+} ions in aqueous solution.[46] Their beads showed selectivity towards Pb^{2+} in a mixture with Cd^{2+}.

(a)

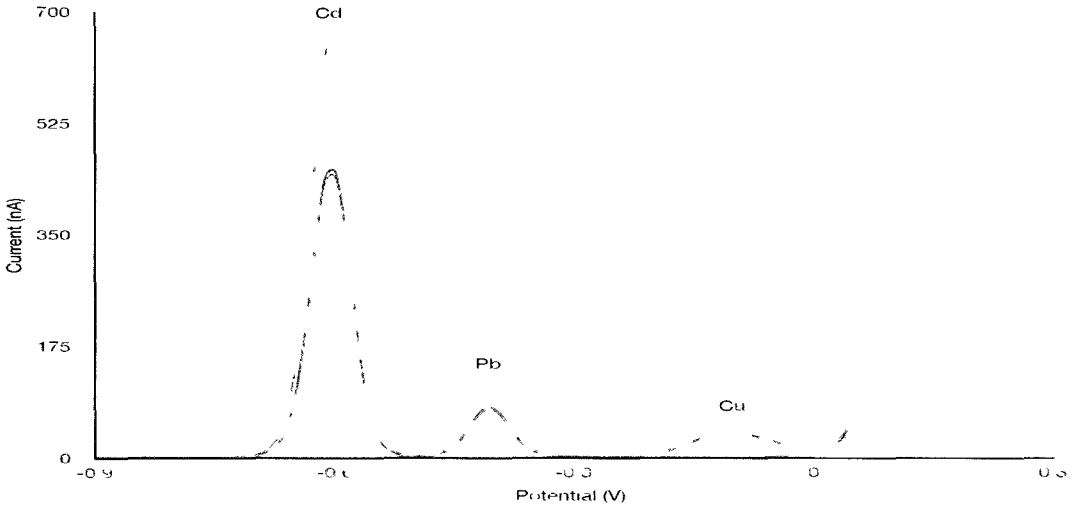
700
525
350
175
0
Current (nA)
Cd
Pb
Cu
Potential (V)

(b)

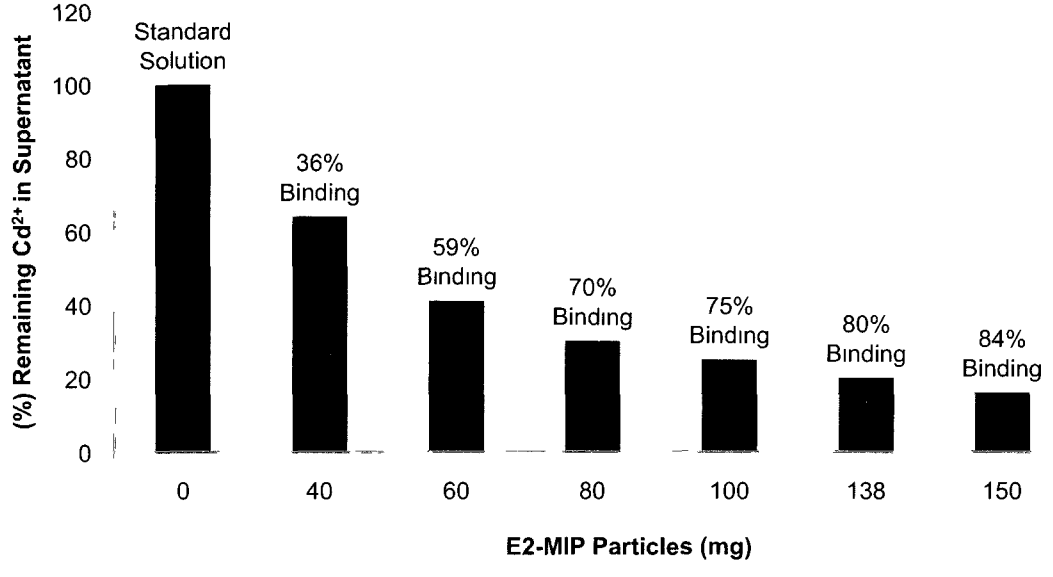
120
100
80
60
40
20
0
(%) Remaining Cd2+ in Supernatant
Standard Solution
36% Binding
59% Binding
70% Binding
75% Binding
80% Binding
84% Binding
0
40
60
80
100
138
150
E2-MIP Particles (mg)

(c)

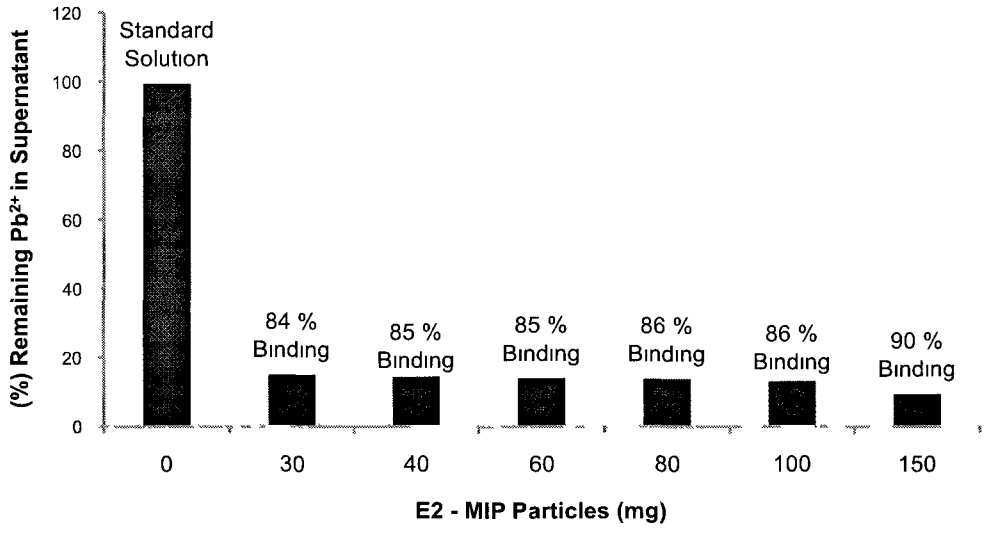

(d)

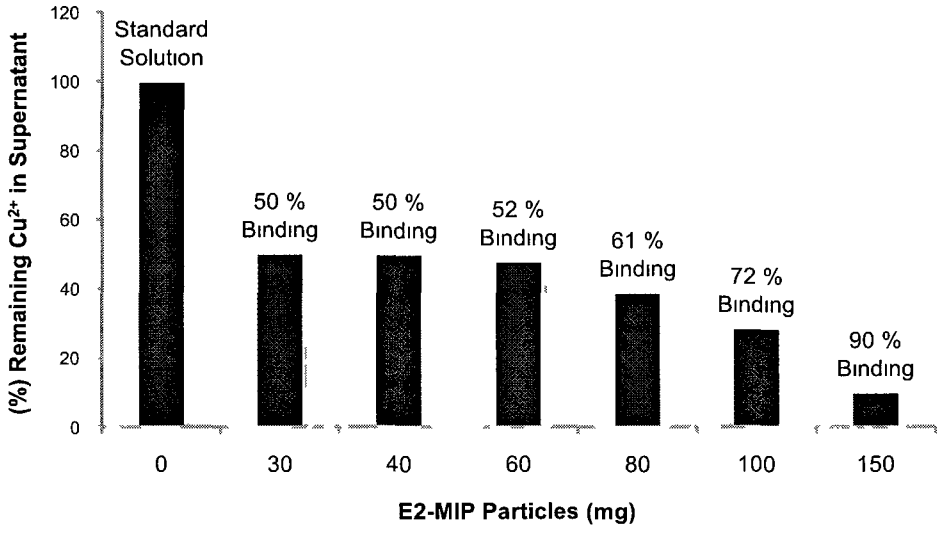

Figure 3 (a) DPASV voltammogram typically exhibited three characteristic peaks for sensitive determination of Cd^{2+}, Pb^{2+} and Cu^{2+} by standard additions % remaining of (b) Cd^{2+}, (c) Pb^{2+} and (d) Cu^{2+} in supernatant after 1 mL of 10^{-5} M standard solution was treated with different weights of E2-MIP particles

3.0.2 Binding of Cd^{2+}, Cu^{2+} and Pb^{2+} onto DCH18C6-MIP particles

DCH18C6-MIP particles were next tested for binding with 10^{-5} M standard solution of Cd^{2+}, Cu^{2+} and Pb^{2+}. As determined from DPASV data not shown here, up to 59±1% of Cd^{2+}, 86±1% of Pb^{2+} and 23±1% Cu^{2+} bound with 150 mg of DCH18C6-MIP particles in 10.7 mL of aqueous solution. Intuitively, DCH18C6 did not bind efficiently with Cd^{2+} and Cu^{2+} due to their small ionic radii (see Table 1 above). By incorporating DCH18C6 within the MIP particles, the size match between the cavity radius of crown ether and the radius of cation is an important parameter governing metal extraction from aqueous solutions. Apparently, Cd^{2+} was a bad match and Cu^{2+} was even worse.

3.0.3 Binding of Cd^{2+}, Cu^{2+} and Pb^{2+} onto DCH18C6-E2-MIP particles

As evidenced by the results presented in Fig. 4, DCH18C6 was successfully incorporated with E2-MIP particles, up to 72%.

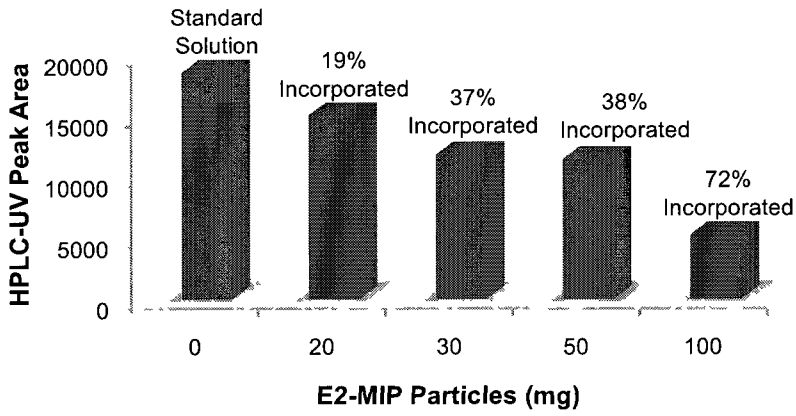

Figure 4 HPLC-UV determination of remaining DCH18C6 in the supernatant after addition of 1 mL of 86 ppm DCH18C6 onto different weights of E2-MIP particles, followed by incubation for 1 hour.

Batches of E2-MIP particles had up to 500 ppm of DCH18C6 incorporated, for binding tests with the 10^{-5} M standard solution of Cd^{2+}, Cu^{2+} and Pb^{2+}. As shown in Fig. 5(a), up to 83±1% of Cd^{2+} bound onto 75 mg of DCH18C6-E2-MIP particles, which was almost the same efficiency (or % binding) as obtained in Fig. 3(b) above using 75 mg of E2-MIP particles (without DCH18C6). The % binding remained almost constant with varying concentrations of DCH18C6 incorporated. This could be explained by a low binding efficiency between DCH18C6 and Cd^{2+}, considering how the crown ether and E2-MIP may share the 83% of Cd^{2+} bound. Next, binding of Pb^{2+} onto E2-MIP particles (without DCH18C6) was 86±2% in Fig. 3(c) above. After 86-500 ppm DCH18C6 was incorporated to form DCH18C6 E2-MIP particles, Pb^{2+} binding increased to 90±3% as shown in Fig. 5(b). One plausible explanation is that the ionic radius for Pb^{2+} is 133 pm (see Table 1 above) and the cavity radius of 18-crown-6 is 130-160 pm. Thus, incorporation of DCH18C6 increased the binding efficiency for Pb^{2+} by a significant 4%.

(a)

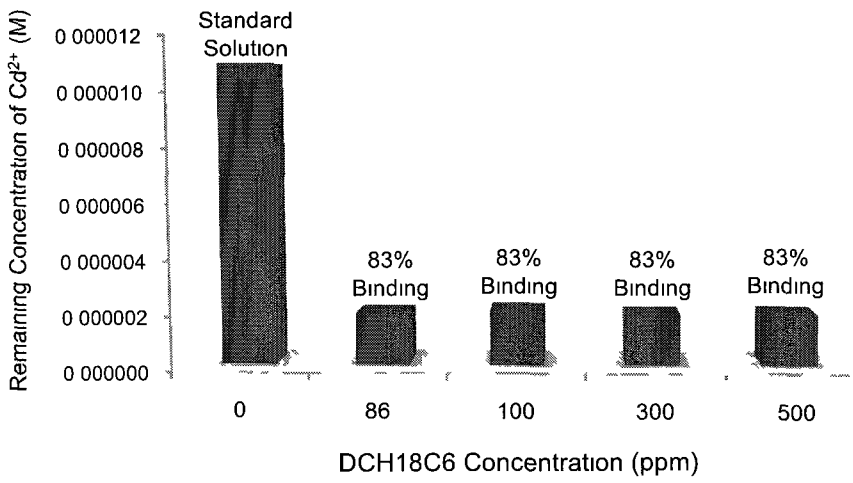

(b)

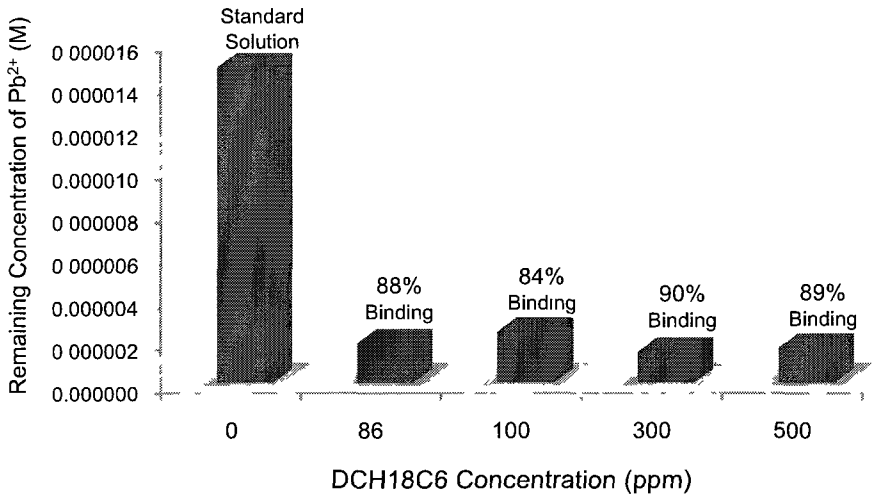

(c)

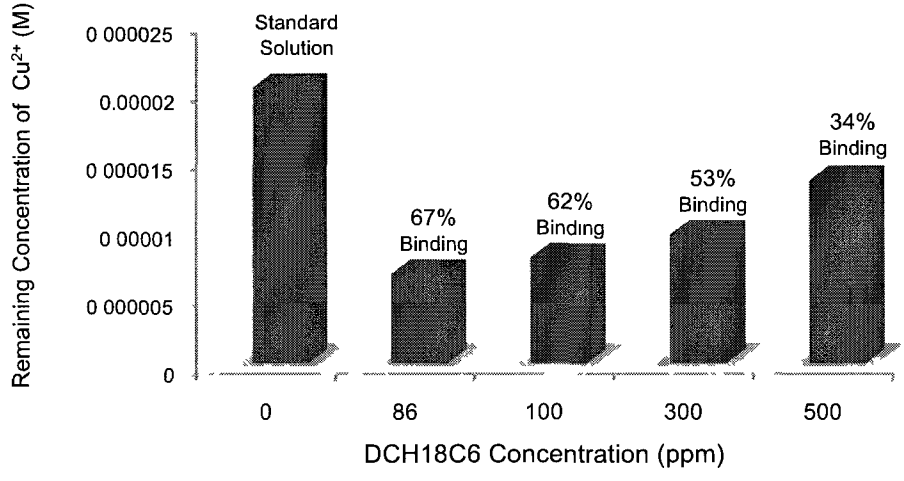

Figure 5 Binding of (a) Cd^{2+}, (b) Pb^{2+}, and (c) Cu^{2+} onto DCH18C6-E2-MIP particles. 0.5 mL of 10^{-5} M standard solution was added to 75 mg of E2-MIP particles incorporated with different concentrations of DCH18C6. After incubation for 1 hour and centrifugation, 0.1 mL of the supernatant was withdrawn for DPASV analysis.

3.0.4 Reversibility of binding by Sr^{2+} competition

E2-MIP particles were used next to investigate the selectivity in binding (for Sr^{2+} against Cd^{2+}, Cu^{2+} and Pb^{2+}). When different concentrations of Sr^{2+} were added to these particles already occupied by Cd^{2+}, Cu^{2+} and Pb^{2+}, their concentrations in the supernatant increased as determined by DPASV analysis. The results in Fig. 6 suggest that Sr^{2+} successfully competed for some binding sites according to the following ion exchange reaction:

$$M^{2+}\text{-E2-MIP} + Sr^{2+} = Sr^{2+}\text{-E2-MIP} + M^{2+} \qquad (1)$$

where M^{2+} could be Cd^{2+}, Pb^{2+} or Cu^{2+}. The effect was prominent for both Cd^{2+} and Cu^{2+}, but only moderate for Pb^{2+}. One plausible explanation is the very similar ionic radii of Sr^{2+} (132 pm) and Pb^{2+} (133 pm), which render the ion exchange less favorable.

(a)

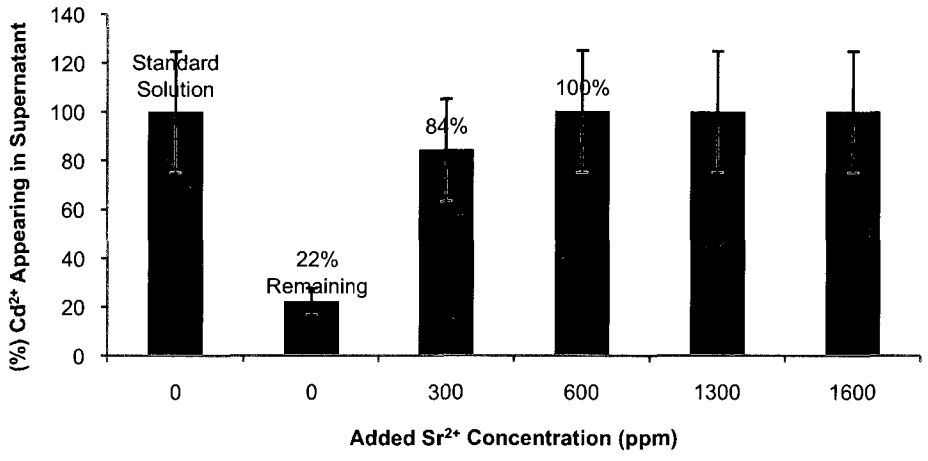

(b)

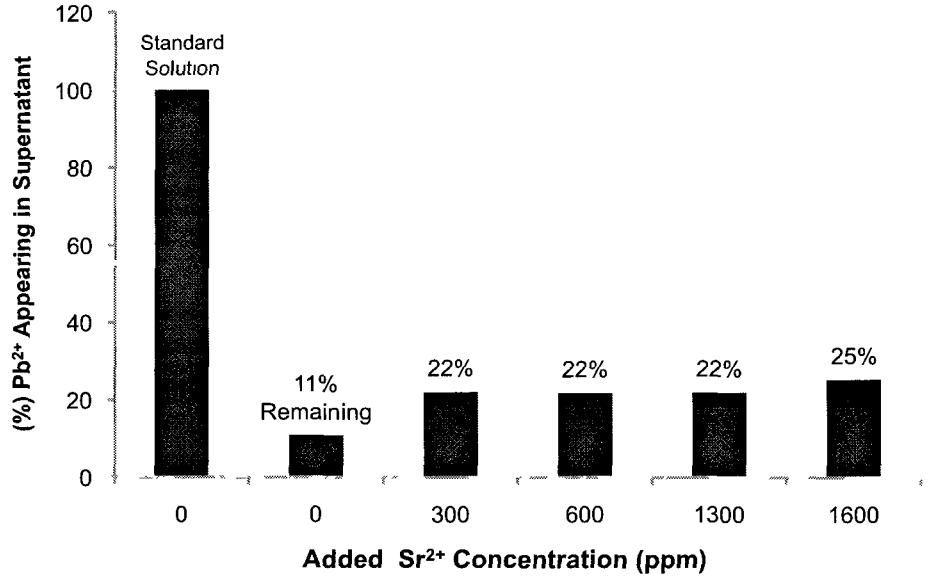

(c)

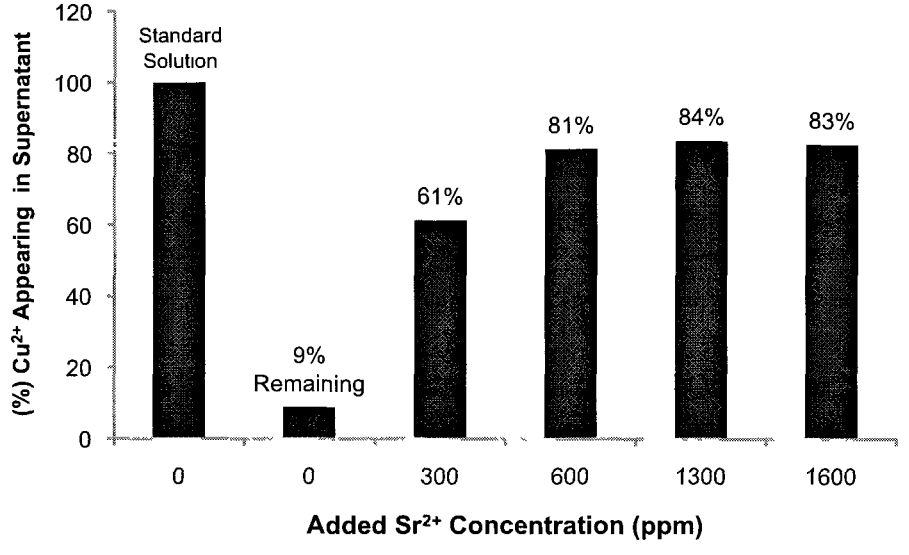

Figure 6 Displacement of (a) Cd^{2+}, (b) Pb^{2+}, and (c) Cu^{2+} from 75 mg of E2-MIP particles (already bound with 10^{-5} M standard solution of Cd^{2+}, Cu^{2+} and Pb^{2+}) by different concentrations of Sr^{2+}, as determined by DPASV analysis of 0.1 mL supernatant after incubation for 1 hour and centrifugation.

The reversibility investigation was repeated using DCH18C6-E2-MIP particles already occupied by Cd^{2+}, Cu^{2+} and Pb^{2+}. These particles had just incorporated 86-500 ppm DCH18C6. As expected, Sr^{2+} successfully competed for some binding sites in a displacement reaction similar to Eq. (1) above. The displacement effect was again prominent for both Cd^{2+} and Cu^{2+}, but only moderate for Pb^{2+}. The % Cd^{2+} appearing in the supernatant increased to 93%, which can be compared with 122% when E2-MIP particles (without DCH18C6) were investigated in Fig. 6(a) above. Also, the % Cu^{2+} appearing in the supernatant increased to 94%. However, the % Pb^{2+} appearing in the supernatant increased to only 20%. Although the ionic radii of Sr^{2+} and Pb^{2+} are very similar (132 and 133 pm respectively), Sr^{2+} is a hard cation and Pb^{2+} is an intermediate cation. Knowing that DCH18C6 is considered as a hard ligand, Sr^{2+} would replace Pb^{2+} to increase its concentration in the supernatant (up to 20% while 80% of Pb^{2+} remained bound to DCH18C6-E2-MIP particles even in the presence of Sr^{2+}).

Rounaghi and Mofazzeli had previously studied complex formation between DCH18C6 and four alkaline earth metal cations using a conductometric method.[47] Their results showed that DCH18C6 formed a 1:1 complex (DCH18C6-Sr^{2+}) with Sr^{2+}, and the order of selectivity was $Ba^{2+} > Sr^{2+} > Ca^{2+} > Mg^{2+}$. Typically hard acids have an electronegativity in the range 0.7 – 1.6 and relatively small size. Hard bases have a high electronegative donor atom (in the range 3.4 – 4).[48]

Our major findings are now summarized in Table 2 for easy comparison. It appears that the increased Cd^{2+}, Pb^{2+} and Cu^{2+} contents in the supernatant both before and after the inclusion of DCH18C6 were primarily due to the E2-MIP rather than the crown ether.

The cavity of DCH18C6 is much larger than the ionic radius of Cu^{2+} (87 pm). Moreover, Cu^{2+} is an intermediate cation and DCH18C6 is considered to be a hard

ligand. Both factors would explain why there was better binding of Cu^{2+} with E2-MIP particles than with DCH18C6-E2-MIP particles (as evidenced by a higher % appearing in the supernatant after addition of 1300 ppm Sr^{2+}). When the concentration of DCH18C6 increased, a decrease in the % binding of Cu^{2+} was actually observed in Fig. 5(c) above.

Table 2 Summary of Cd^{2+}, Pb^{2+} and Cu^{2+} binding results for E2-MIP and DCH18C6-E2-MIP particles, followed by displacement using Sr^{2+}. % binding results for DCH18C6-MIP particles are included for quick reference.

	Particles	% Binding*	% Remaining in supernatant before addition of 1300 ppm Sr^{2+}	% Appearing in supernatant after addition of 1300 ppm Sr^{2+}
Cd^{2+}	E2-MIP	84 ± 4	16 ± 1	100 ± 5
	DCH18C6-E2-MIP	83 ± 4	17 ± 1	93 ± 4
	DCH18C6-MIP	59 ± 3		
Pb^{2+}	E2-MIP	89 ± 4	11 ± 0 6	22 ± 1
	DCH18C6-E2-MIP	90 ± 5	10 ± 0 6	21 ± 1
	DCH18C6-MIP	87 ± 4		
Cu^{2+}	E2-MIP	98 ± 3	2 ± 0 2	84 ± 4
	DCH18C6-E2-MIP	96 ± 3	4 ± 0 2	94 ± 5
	DCH18C6-MIP	23 ± 1		

* % binding = 100% - % remaining in supernatant

3.0.5 Reversibility of binding by Y^{3+} competition

Furthermore, Y^{3+} was added to compete for the binding sites already occupied by Cd^{2+}, Cu^{2+} and Pb^{2+} inside E2-MIP particles. As shown in Fig. 7, the concentrations of all three metal ions in the supernatant increased with the addition of more Y^{3+}. Cd^{2+} was displaced easily from the E2-MIP particles by Y^{3+}, Cu^{2+} was displaced with reluctance, while Pb^{2+} was hardly displaced. By comparison, Fig. 5 above demonstrated that Sr^{2+} was able to displace Cd^{2+} more easily and Cu^{2+} much more readily. It is logical to deduce that the E2-MIP particles are selective in binding for Sr^{2+} over Y^{3+}. However, Y^{3+} seemed to be better able to displace Pb^{2+} than Sr^{2+} probably due to its higher ionic charge.

(a)

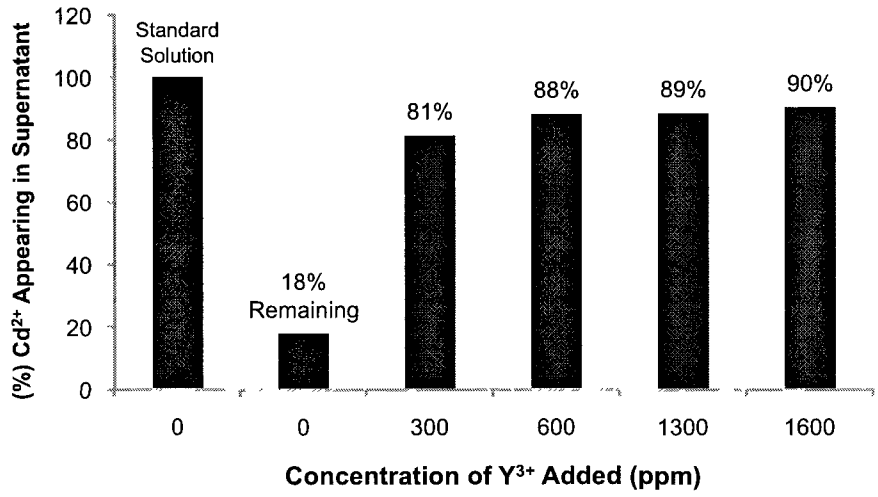

(b)

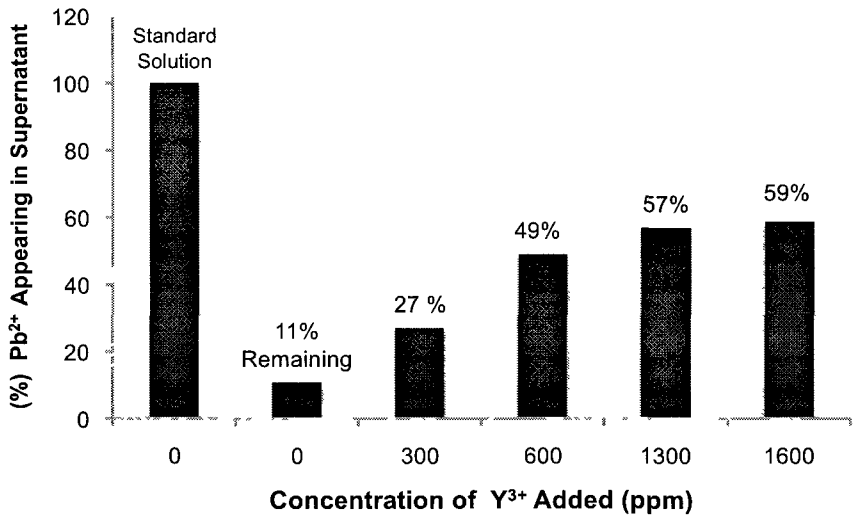

(c)

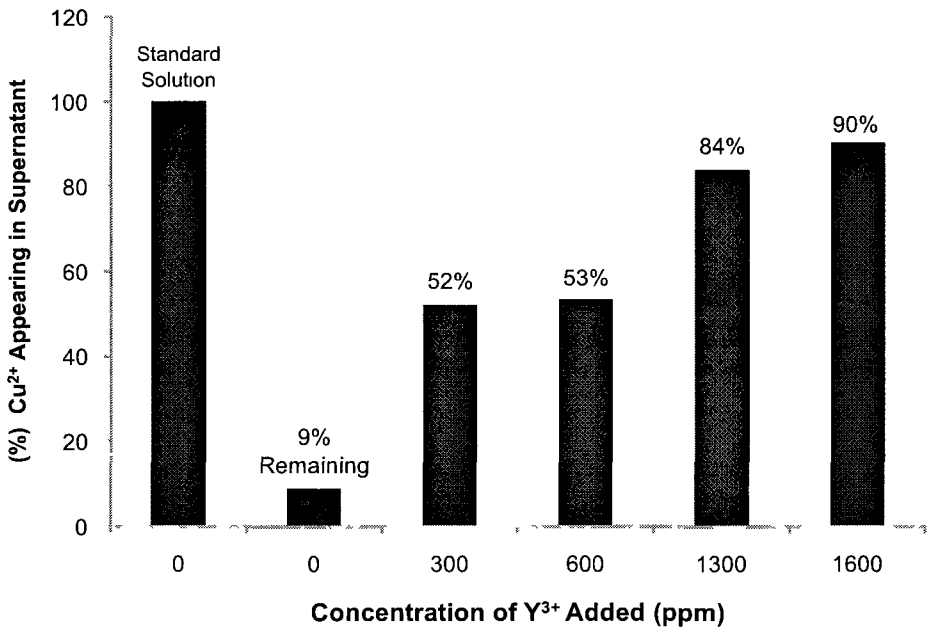

Figure 7 Displacement of (a) Cd^{2+}, (b) Pb^{2+}, and (c) Cu^{2+} from 75 mg of E2-MIP particles (already bound with 10^{-5} M standard solution of Cd^{2+}, Cu^{2+} and Pb^{2+}) by different concentrations of Y^{3+}, as determined by DPASV analysis of 0.1 mL supernatant after incubation for 1 hour and centrifugation.

The reversibility investigation was repeated using DCH18C6-E2-MIP particles already occupied by Cd^{2+}, Cu^{2+} and Pb^{2+} inside the binding sites As expected, Y^{3+} successfully competed for some binding sites in a displacement reaction Again, Cd^{2+} was displaced easily from the DCH18C6-E2-MIP particles by Y^{3+}, Cu^{2+} was displaced with reluctance, while Pb^{2+} was hardly displaced This behavior is similar to that of Sr^{2+} discussed above As summarized in Table 3, all results for % remaining in the supernatant after addition of 1300 ppm Y^{3+} suggest that DCH18C6 is a ligand with stronger binding affinity for Y^{3+} (over and above those for Cd^{2+}, Cu^{2+} and Pb^{2+}) just like Sr^{2+} Note that Y^{3+} is a trivalent cation that bound to E2-MIP more strongly than Pb^{2+} Hence, 57% of Pb^{2+} appeared in the supernatant (compared to only 22% of Sr^{2+})

Table 3 Summary of Cd^{2+}, Pb^{2+} and Cu^{2+} binding results for E2-MIP and DCH18C6-E2-MIP particles, followed by displacement using Y^{3+} % binding results for DCH18C6-MIP particles are included for quick reference

	Particle's Description	% Binding*	% Remaining in supernatant before addition of 1300 ppm Y^{3+}	% Remaining in supernatant after addition of 1300 ppm Y^{3+}
Cd^{2+}	E2-MIP	84 ± 4	16 ± 1	88** ± 5 (cf *** 100 for Sr^{2+})
	DCH18C6-E2-MIP	83 ± 4	17 ± 1	99 ± 6 (cf 93 for Sr^{2+})
	DCH18C6-MIP	59 ± 3		
Pb^{2+}	E2-MIP	89 ± 5	11 ± 0 6	57 ± 3 (cf 22 for Sr^{2+})
	DCH18C6-E2-MIP	90 ± 5	10 ± 0 5	27 ± 2 (cf 21 for Sr^{2+})
	DCH18C6-MIP	87 ± 4		
Cu^{2+}	E2-MIP	98 ± 5	2 ± 0 1	84** ± 4 (cf 84 for Sr^{2+})

	DCH18C6-E2-MIP	96 ± 5	4 ± 0.2	98 ± 5 (cf. 94 for Sr^{2+})
	DCH18C6-MIP	23 ± 1		

* % binding = 100% - % remaining in supernatant
** increased to 90% when Y^{3+} was added up to 1600 ppm
*** = confer (compare with)

3.1. Binding Studies of Strontium onto Molecularly Imprinted Polymer

The main goal of this research is to develop a rapid bioassay method for strontium measurements, with minimal interference by yttrium, during emergency urinalysis. A molecularly imprinted polymer, compromised with dicyclohexano-18-crown-6 ether, was synthesized and studies on optimization for ^{90}Sr quantization were developed. From this simple and cost-effective synthesis, the resultant MIP particles are equipped with DCH18C6 sites that will selectively bind Sr^{2+} in urine samples. These particles can be stored dry, without any significant loss of DCH18C6 or lengthy reconditioning, for emergency use. The method evaluation was done under gamma spectroscopy (^{85}Sr) and liquid scintillation counter (^{90}Sr /^{90}Y), analysis.

3.1.1 Binding of Sr^{2+} onto DCH18C6-E2-MIP particles (as determined by AES)

Since DPASV cannot be used directly to determine Sr^{2+}, binding of Sr^{2+} onto DCH18C6-E2-MIP particles was studied further by atomic emission spectrometry (AES) at 407.7 nm or 421.5 nm. Experimental results, Figures 8 and 9, showed dependency of % binding on increasing ionic strength. Apparently, Sr^{2+} binding onto the DCH18C6-E2-MIP particles may involve outer-sphere complex formation.[49]

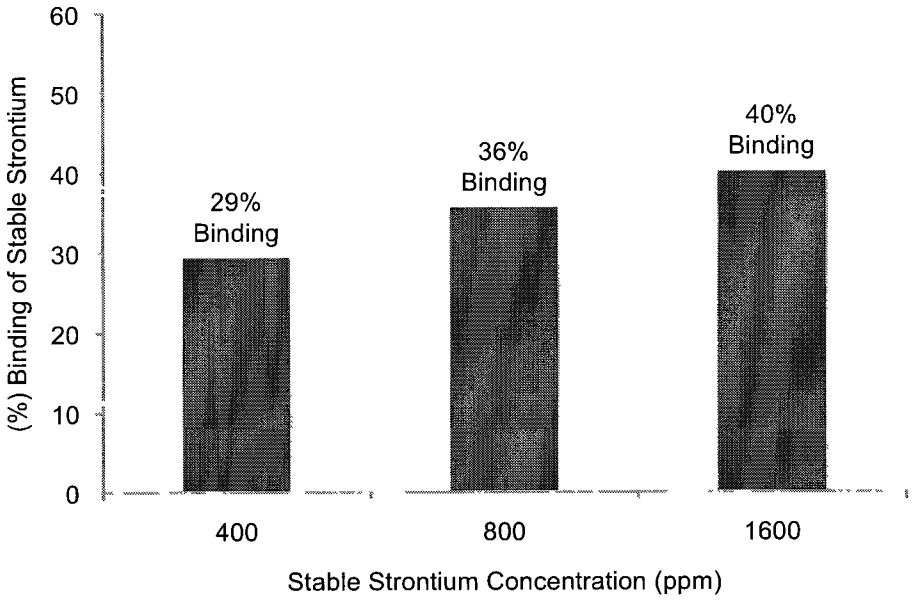

Figure 8 Effect of stable strontium concentration (ppm) onto 150 mg DCH18C6-E2-MIP particles in DDW matrix at pH 4.1.

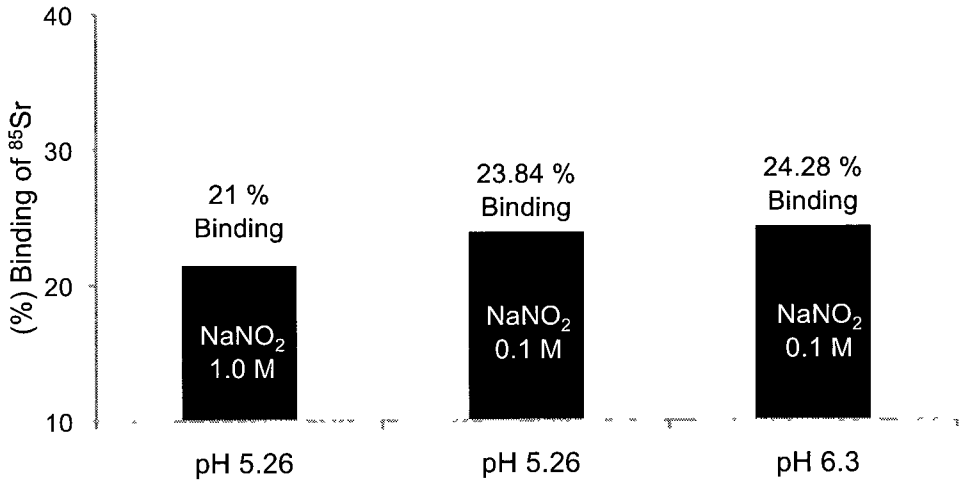

Figure 9 pH and ionic strength effect on ^{85}Sr uptake onto 150 mg DCH18C6-E2-MIP particles in DDW matrix.

3.1.2 Comparison on ^{85}Sr uptake onto E2-MIP incubated with various concentrations of DCH18C6

As described earlier, dicyclohexano-18-crown-6 is a ligand with strong binding affinity for Sr^{2+} due to the cavity match of DCH18C6 with the ionic radii of Sr^{2+}. In this study the ^{85}Sr uptake onto E2-MIP incorporated with various amount of dicyclohexano-18-crown-6 was examined. Experimental results showed that the % binding increased with increasing the concentration of DCH18C6 up to 43 mM. After DCH18C6 43 mM concentration, the binding percent of ^{85}Sr onto MIP particles decreases. This might be explained by the lack of ligand (DCH18C6) interaction with E2-MIP particles due to steric crowding around the binding sites, therefore loss of recognition and limited access of ^{85}Sr to the crown ether cavity.

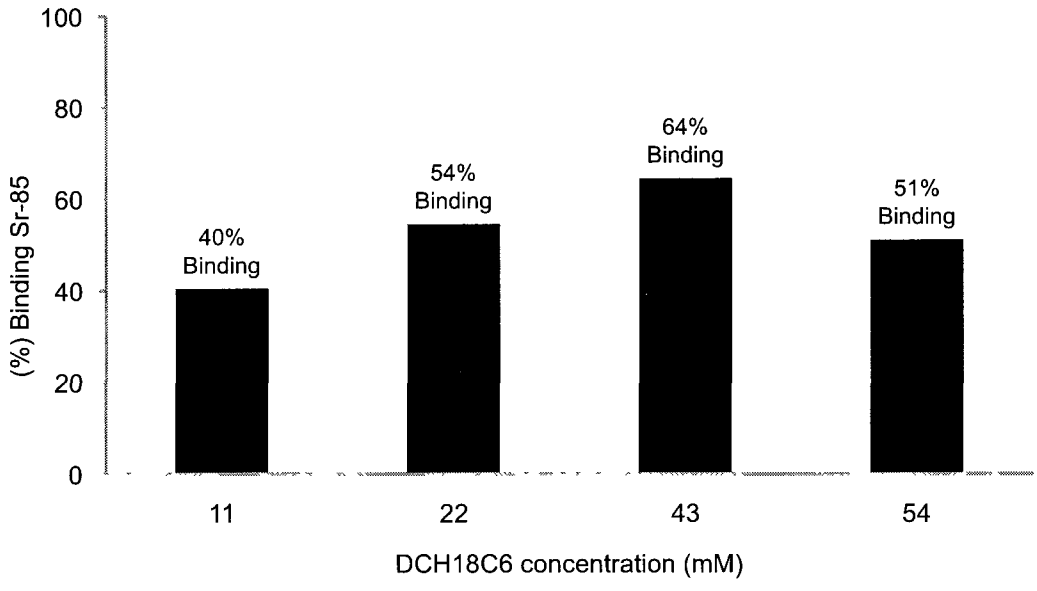

Figure 10 Effect of DCH18C6 concentration (mM) on ^{85}Sr uptake by 300 mg DCH18C6-E2-MIP particles.

3.1.3. ^{85}Sr uptake onto DCH18C6-MIP particles

Binding of $^{85}Sr^{2+}$ was next studied using DCH18C6-MIP particles at pH 6.3 and $NaNO_2$ 0.1M. The most promising result, for 300 mg of DCH18C6-MIP particles impregnated with 43 mM DCH18C6, showed 87% binding of $^{85}Sr^{2+}$.

3.1.4. FTIR spectra of E2-MIP, DCH18C6-MIP and DCH18C6-E2-MIP particles

The three types of MIP particles have similar IR spectra, indicating commonality in their backbone structures, as shown in Fig. 11 (a). Absorption peaks due to carboxyl OH stretch (~3500 cm^{-1}), C=O stretch (~1730 cm^{-1}), C-O stretch (~1260 cm^{-1}) and C-H vibrations (~756, ~1390, ~1460, and ~2956 cm^{-1}) were observed as expected.[50]

(a)

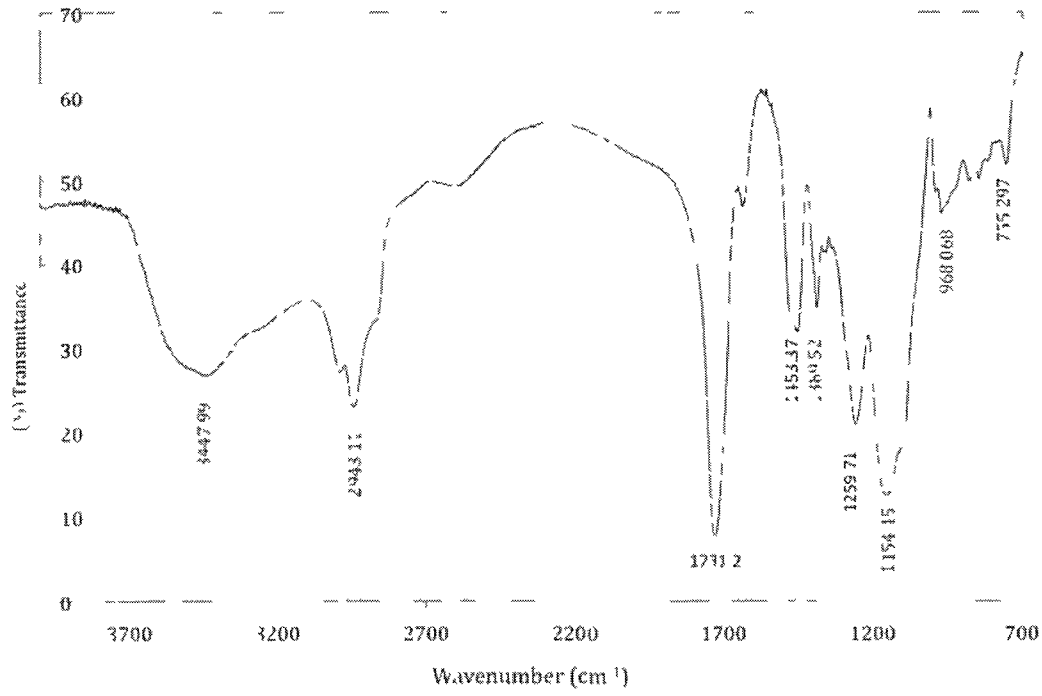

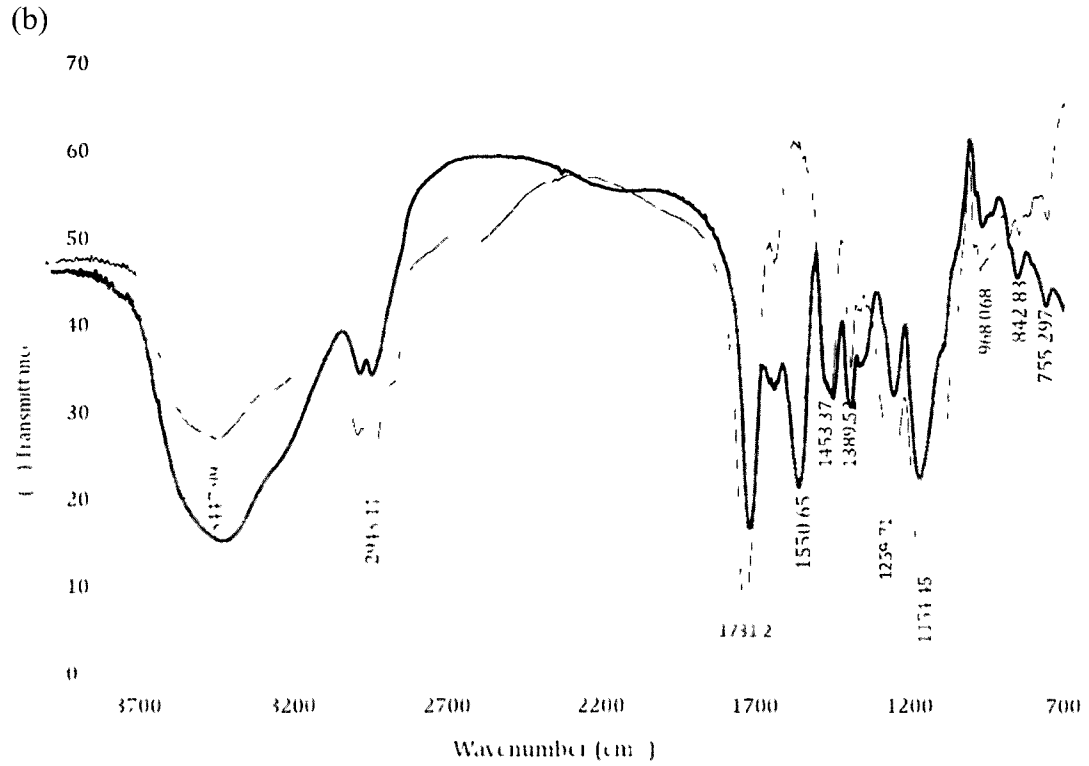

Figure 11 The FTIR spectra of (a) E2-MIP, DCH18C6-MIP and DCH18C6-E2-MIP particles and (b) NaOH treated DCH18C6-MIP (red) and DCH18C6-MIP particles

In the FTIR spectrum of the NaOH-treated DCH18C6-MIP particles (Figure 11 b, red), the broad peak at ≈ 3448 cm^{-1} suggested that the surface was rich in hydroxyl groups.[51] NaOH treatment results, in shape changes of the bands attributed to C=O, C–O and C–O–C, indicate creation of oxygenated groups, which in turn increase surface polarity and improve hydrophilicity.[52] FTIR results clearly show a new peak around 1560 cm^{-1}, which is representative of -COOH. This peak increases as the NaOH concentration increase.[53]

3.1.5 Effect of pH on ^{90}Sr and ^{90}Y uptake

As shown in Figure 12, the % binding results for $^{90}Sr^{2+}$ and $^{90}Y^{3+}$ onto DCH18C6-MIP particles were found to be pH dependent. At pH levels below 5, the % binding was low probably due to $-COO^-$ binding sites being protonated. The neutral range of pH 6.3-6.8 seemed to be optimal for both adequate binding of strontium and moderate interference by yttrium. At pH levels above 8, the high % binding of yttrium actually exceeded that for strontium.

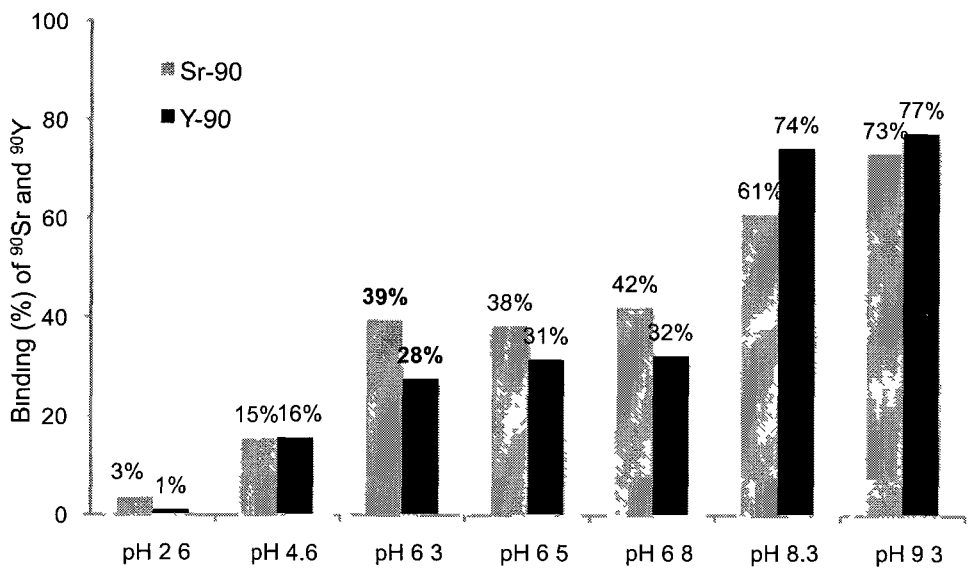

Figure 12 pH effect on $^{90}Sr^{2+}$ and $^{90}Y^{3+}$ binding onto 150 mg of DCH18C6-MIP particles at ionic strength of 0 1 M $NaNO_2$

3.1.6 Effect of ionic strength of different salts on strontium uptake

The effect of ionic strength on strontium binding onto DCH18C6-MIP particles was investigated at pH 6.3, using ^{85}Sr as a tracer. Experimental results showed that the % binding increased with increasing ionic strength (provided by $NaNO_2$) up to 0.3 M. This was probably due to the formation of an outer-sphere complex with Sr^{2+} bound on the particles.[54] Outer sphere complex formation involves interaction between the $^{90}Sr^{2+}$ hexa-aquo cation and the MIP fuctional groups. Water molecules remain between $^{90}Sr^{2+}$ and the MIP binding sites through electrostatic attractions or hydrogen bonding,[55] which are influenced by the ionic strength.[56,57]

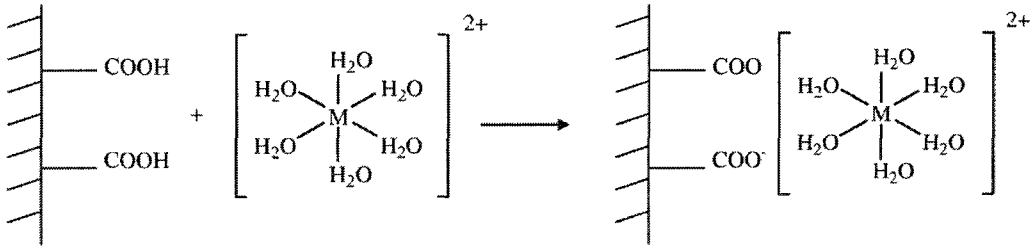

Figure 13 Outer-sphere metal complex formation for a divalent hexa-aquo cation.[55]

It had previously been reported that Hofmeister salts interacted directly with polymers, which might even be specifically bonded with Hofmeister ions having a strong salting-in effect (Mracek et al. 2008). As shown in Figure 14, $NaNO_2$ resulted in 97% binding which was higher than $NaNO_3$ and NaI when they were compared at the same ionic strength of 0.3 M. These results apparently followed the Hofmeister series of

anions in order of decreasing lipophilicity: $I^- > NO_3^- > NO_2^-$.[58] Maximal binding of 97% was attained, using $NaNO_2$ at an ionic strength of 0.3 M at pH 6.3 for DCH18C6-MIP particles.

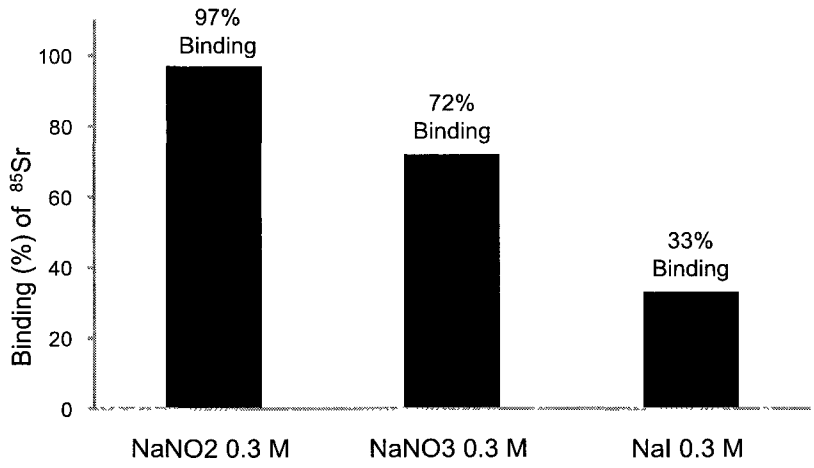

Figure 14 Effects of different Hofmeister salts on ^{85}Sr binding onto 500 mg of DCH18C6-MIP particles at pH 6.3 in urine matrix.

3.1.7 Ionic strength and pH effect on NaOH treated DCH18C6-MIP particles

The pH of urine is close to neutral. Based on individual eating habits, the ionic strength of urine ranges from 0.1 to 0.5 with an average of 0.32. Development of a MIP particle with similar ^{90}Sr uptake in a range of ionic strengths is beneficial for an emergency urinassay.

Figure 16(a) and b shows how well NaOH treatment of DCH18C6-MIP particles resulted in significantly higher % binding of strontium, and yttrium. By treating the particles with NaOH, the number of negatively charged $-COO^-$ binding sites on the MIP particles was increased due to deprotonation.

It is interesting to notice that the strontium binding remained essentially the same (98±1%) for all ionic strengths ranging from 0.1 to 0.5 M and pH range 0.82 – 7.24. Such a lack of ionic strength dependence has previously been inferred to indicate inner-sphere complexation[54] between the cation and the treated DCH18C6-MIP particles, where $^{90}Sr^{2+}$ is covalently bonded to the MIP binding sites.[55]

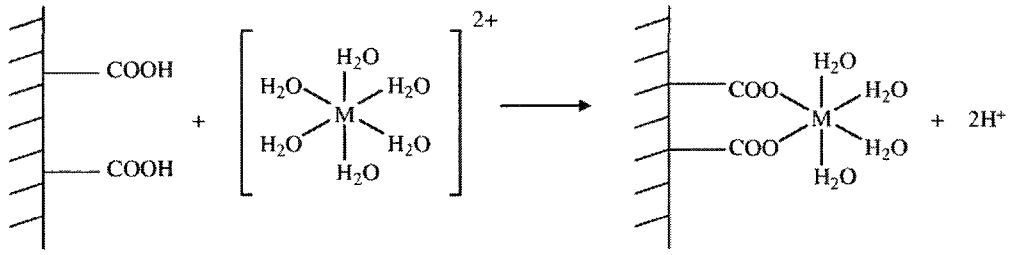

Figure 15 Inner-sphere surface metal complex formation for a divalent hexa-aquo cation.[55]

(a)

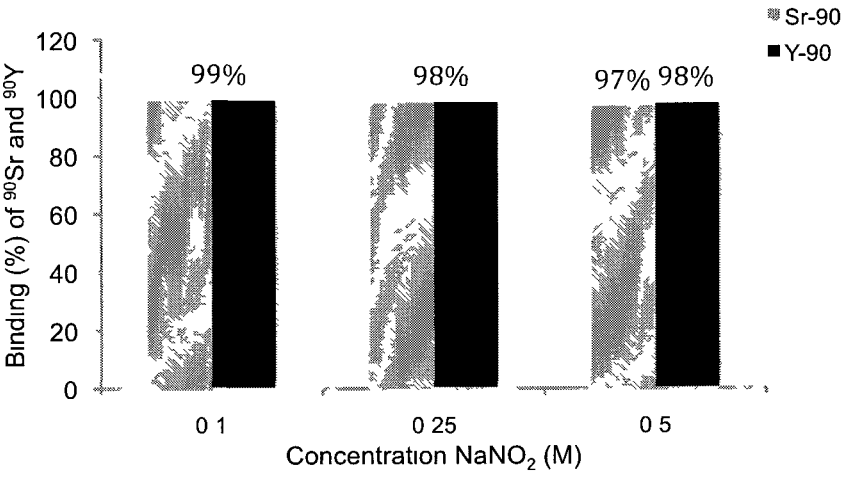

(b)

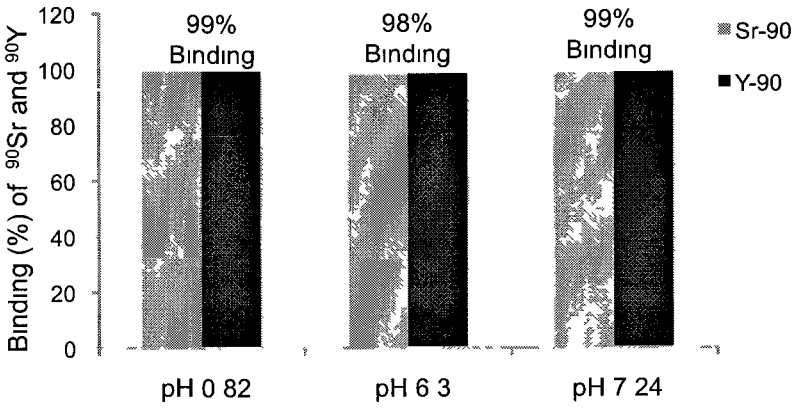

Figure 16 ^{90}Sr and ^{90}Y binding onto 500 mg of NaOH-treated DCH18C6-MIP particles in urine matrix (a) at pH 6 3 and different ionic strengths provided by $NaNO_2$ and (b) different pHs

3.1.8. Amount (weight) of DCH18C6-MIP particles

Figure 17 shows how much ^{85}Sr bound onto different amounts of DCH18C6-MIP particles. The highest % binding was obtained using 500 mg of DCH18C6-MIP particles, as expected by binding isotherms in general. It is noteworthy to mention that the ^{85}Sr sample solution also contained stable strontium (50 μg mL^{-1}) as carrier. This amount of stable strontium carrier in each urine sample was significantly higher than that typically found in human urine (0.14 μg mL^{-1})[59] because the ^{85}Sr level had to be above the quantification limit of gamma spectroscopy. Such abundance of stable Sr^{2+} inevitably necessitated the use of more MIP particles to achieve quantitative uptake of ^{85}Sr.

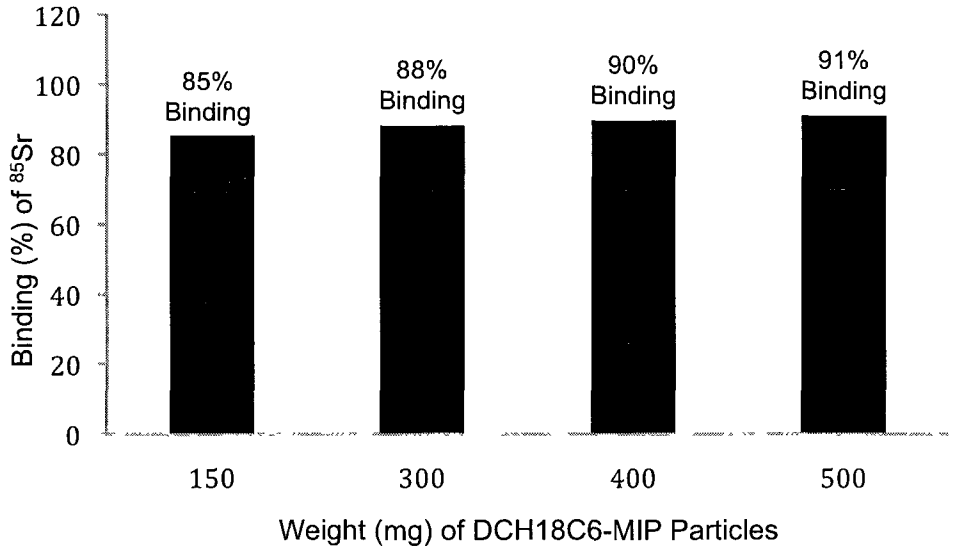

Figure 17 ^{85}Sr binding onto different amounts of DCH18C6-MIP particles in urine matrix, at pH 6.3 and ionic strength of 0.3 M $NaNO_2$.

3.2. Study on ^{90}Y precipitation

Preconditioning and sample purification by precipitation method is based on the differences in solubility of their compounds in aqueous solutions. The solid material produced from the precipitation process is in equilibrium with ions in the solution. The solubility product K_{sp}, can describe this equilibrium. The smaller the solubility product, the more difficult is to solve the precipitate in the solution.[60]

The precipitation of ^{90}Y was studied on urine samples spiked with ^{90}Sr and ^{90}Y mixture, in the presence of KIO_3, H_5IO_3 and TiO_2 separately. Investigation on ^{90}Y precipitation by H_5IO_6 was adapted from a previously developed method by Hector et al. (2002).[61] Periodic acid or iodic(VII) acid is an oxoacid of iodine having chemical formula HIO_4 or H_5IO_6. In dilute aqueous solution, periodic acid exists as discrete hydronium (H_3O^+) and metaperiodate (IO_4^-) ions. When more concentrated, orthoperiodic acid, H_5IO_6, is formed; this dissociates into hydronium and orthoperiodate (IO_6^{5-}) ions. In practice, the metaperiodate and orthoperiodate ions co-exist in a pH-dependent chemical equilibrium:[62]

$$IO_4^- + 6\ H_2O \rightleftharpoons IO_6^{5-} + 4\ H_3O^+$$

As described by Hector et al., periodic acid behaves as a strong O^- donor chelates[3], the reaction of yttrium ion with H_5IO_6 in weakly acid solution produced $Y(H_2O)_3\{IO_4(OH)_2\}$ precipitation.[61] Figure 18 shows the results obtained in the presence of periodic acid, at pH 5.6, 95% of ^{90}Y is removed from the urine sample by precipitation. The back draw

through this method is the 64% co-precipitation of ^{90}Sr for the strontium and yttrium separation.

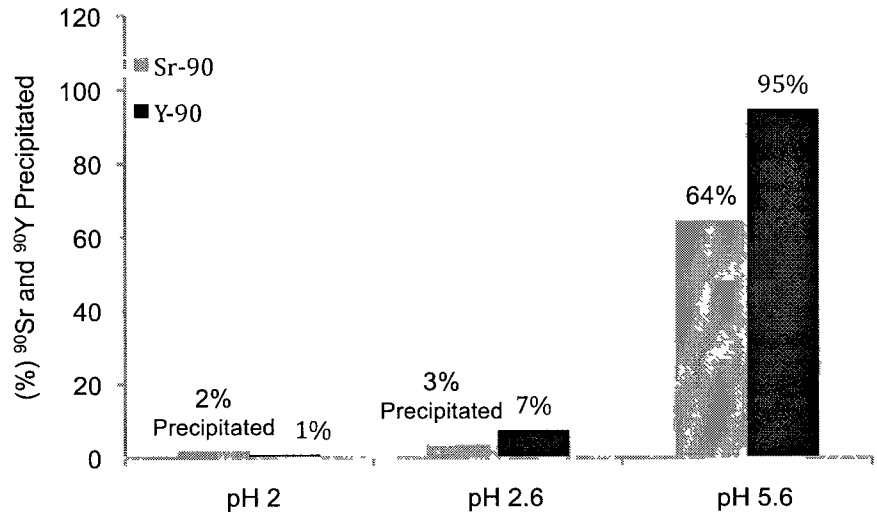

Figure 18 pH effect on ^{90}Sr and ^{90}Y precipitation with H_5IO_6 (1:1 molar ratio with yttrium) in urine matrix.

Figure 19 shows the results for yttrium and strontium precipitation while using KIO_3. The results showed the precipitation of yttrium is accompanied with a high amount (%) co-precipitation of strontium. In the methods described, the co-precipitation of strontium is a disadvantage for the strontium and yttrium separation.

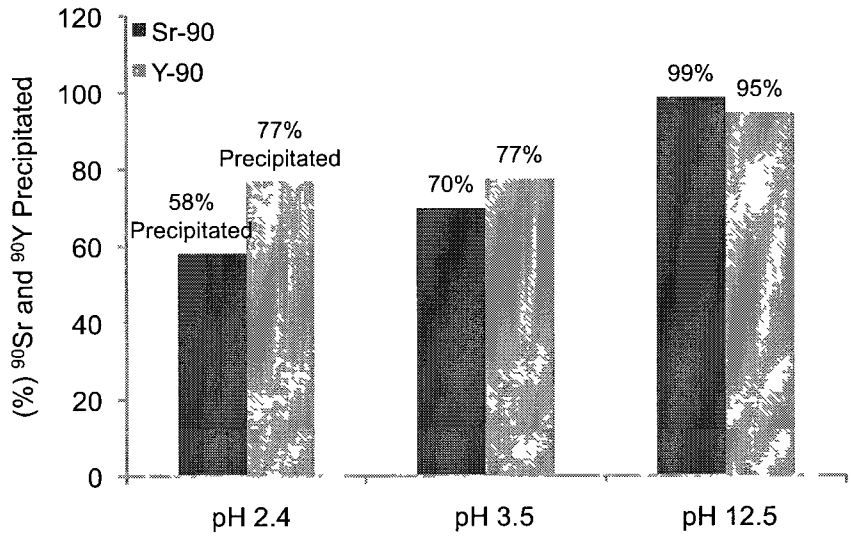

Figure 19 pH effect on ^{90}Sr and ^{90}Y precipitation with KIO_3 (0.5 mol L^{-1}) in urine matrix.

As rapid bioassay methods for strontium would require minimal interference by yttrium, TiO_2 was assessed as a sorbent to preferentially adsorb ^{90}Y. Titanium oxide belongs to the family of tetravalent element oxides. These hydrous oxides show acidic properties due to the surface hydroxyl groups.[63] Titanium dioxide, with a low solubility in urine samples, has been found to be a strong sorbent for cations especially at acidic pH levels.[64] Figures 20 and 21 show the pH effect, amount of TiO_2 used on the adsorption of $^{90}Sr^{2+}$ and $^{90}Y^{3+}$, respectively. The results showed that at pH 6.4 ±1, 85% of ^{90}Y is adsorbed onto the solid TiO_2 together with only 26% of ^{90}Sr. Sorption affinity was strongly related to the radius and charge of each cation.

Wesolowski et al. (2008) had previously reported that the affinity of TiO_2 for trivalent cations is many orders of magnitude larger and than that for divalent cations.[65] Any yttrium adsorbed onto the titanium oxide surface could be removed from the urine

sample by centrifugation, thereby minimizing interference with the subsequent ^{90}Sr urine bioassay. After up to 94% of ^{90}Y and down to 29% of ^{90}Sr were removed by precipitation, the remaining ^{90}Sr and ^{90}Y in urine matrix could be added to 500 mg DCH18C6-MIP particles.

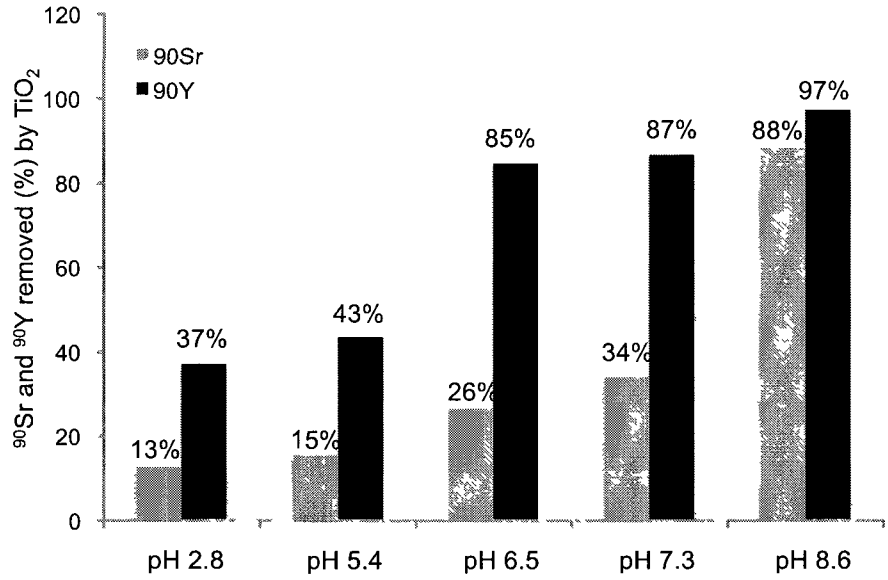

Figure 20 pH effect on ^{90}Sr and ^{90}Y precipitation with TiO_2 (0.05 mol L^{-1}) in urine matrix.

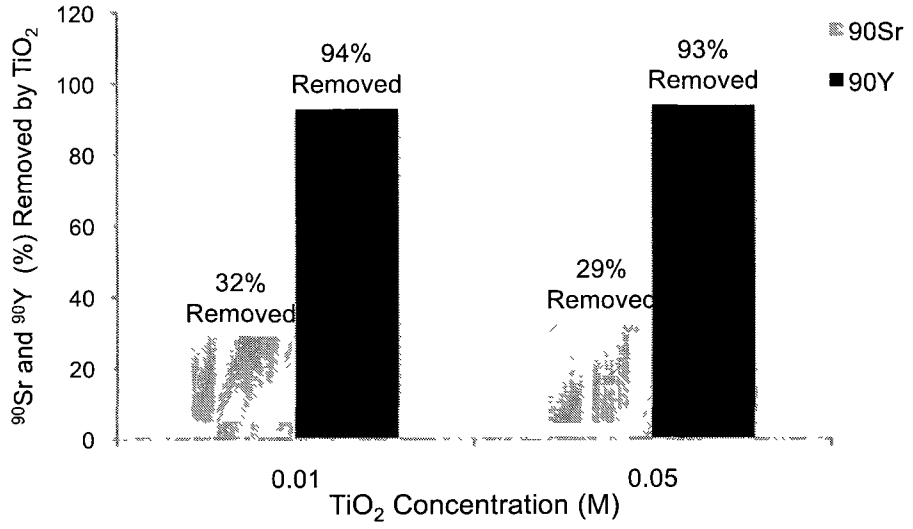

Figure 21 ^{90}Sr and ^{90}Y (%) removed by precipitation with TiO_2 (0.01 and 0.05 mol L^{-1}) at pH 6.3 in urine matrix.

Literatures have quoted pH 5.8 – 6.8 as isoelectrioc point (point of zero charge) for TiO_2.[66,67,68] Adsorption of metal ions onto TiO_2 is an endothermic process, which means adsorption amount increases with increasing in temperature.[69]

It was found that hydroxyl ions in aqueous solution are consumed by the colloidal semiconductor surface of TiO_2/electrolyte interferance.[68] The sorption of metal ions onto TiO_2 surface follows both chemisorption and physisorption mechanisms.[66]

When pH is below PZC, the TiO_2 surface is positively charged in the form of $Ti\text{-}OH^{1/2+}$.[66] The M^{2+} binding can be explained through chemisorption through formation of chemical bonds, where the metal cation will bind to the TiO_2 surface bridging oxygen.[66] At pH is above PZC, the TiO_2 surface is negatively charged in the form of $Ti\text{-}OH^{1/2-}$. The binding of M^{2+} onto the TiO_2 surface will follow both chemisorption and

physisorption by electrostatic force between the oppositely charged adsorbate and adsorbent.[66]

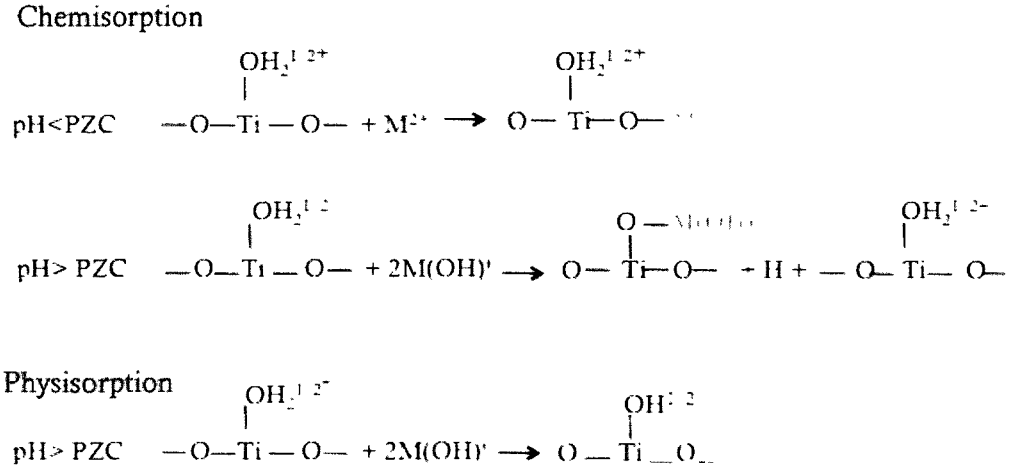

Figure 22 Adsorption processes onTiO_2 surface: chemisorption and physisorption [66]

3.3. Direct LSC measurement of ^{90}Sr bound to DCH18C6-MIP particles

Liquid scintillation spectra could then be obtained for both ^{90}Sr/^{90}Y bound to DCH18C6-MIP particles in cocktail suspension and ^{90}Sr/^{90}Y in supernatant. Figure 23 shows that results in (a,b) for the amount of ^{90}Sr/^{90}Y bound to DCH18C6-MIP particles was in good agreement with those in (c, d) for ^{90}Sr/^{90}Y remaining in the supernatant. The particles were obviously good for selective SPE of ^{90}Sr in urine bioassay.

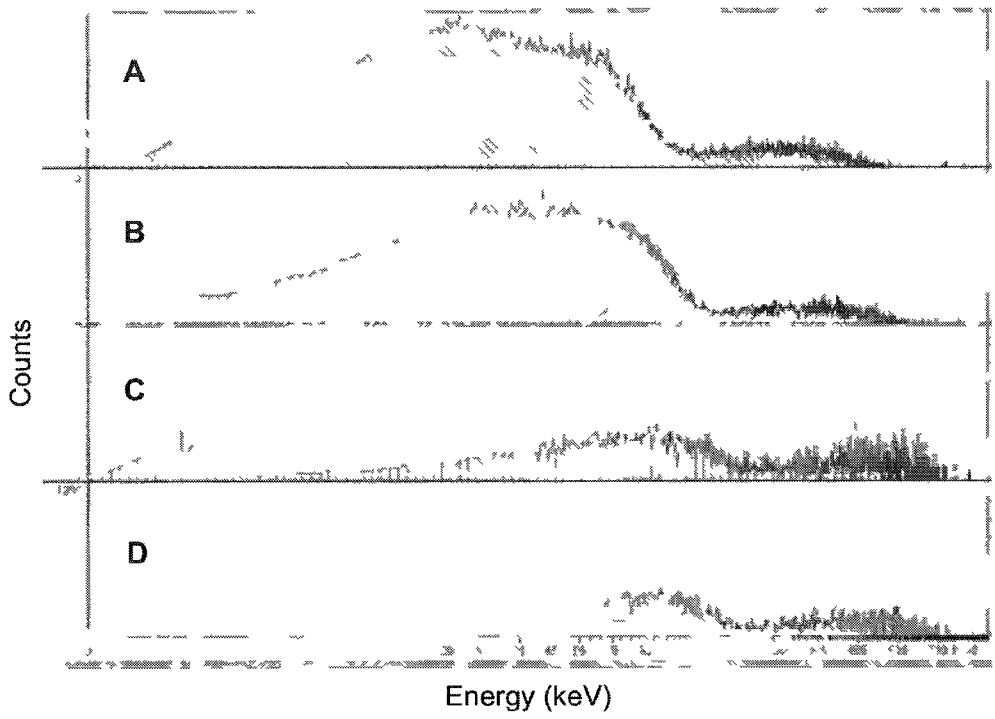

Figure 23 After up to 94% of ^{90}Y and down to 29% of ^{90}Sr were removed by precipitation, the remaining ^{90}Sr and ^{90}Y in urine matrix was added to 500 mg DCH18C6-MIP particles (at pH 6 3 and ionic strength of 0 3 M $NaNO_2$) Liquid scintillation spectra for (a, b) $^{90}Sr/^{90}Y$ bound to DCH18C6-MIP particles in cocktail suspension, and (c, d) $^{90}Sr/^{90}Y$ remaining in supernatant

3.4. Summarized method for ^{90}Sr urine bioassay

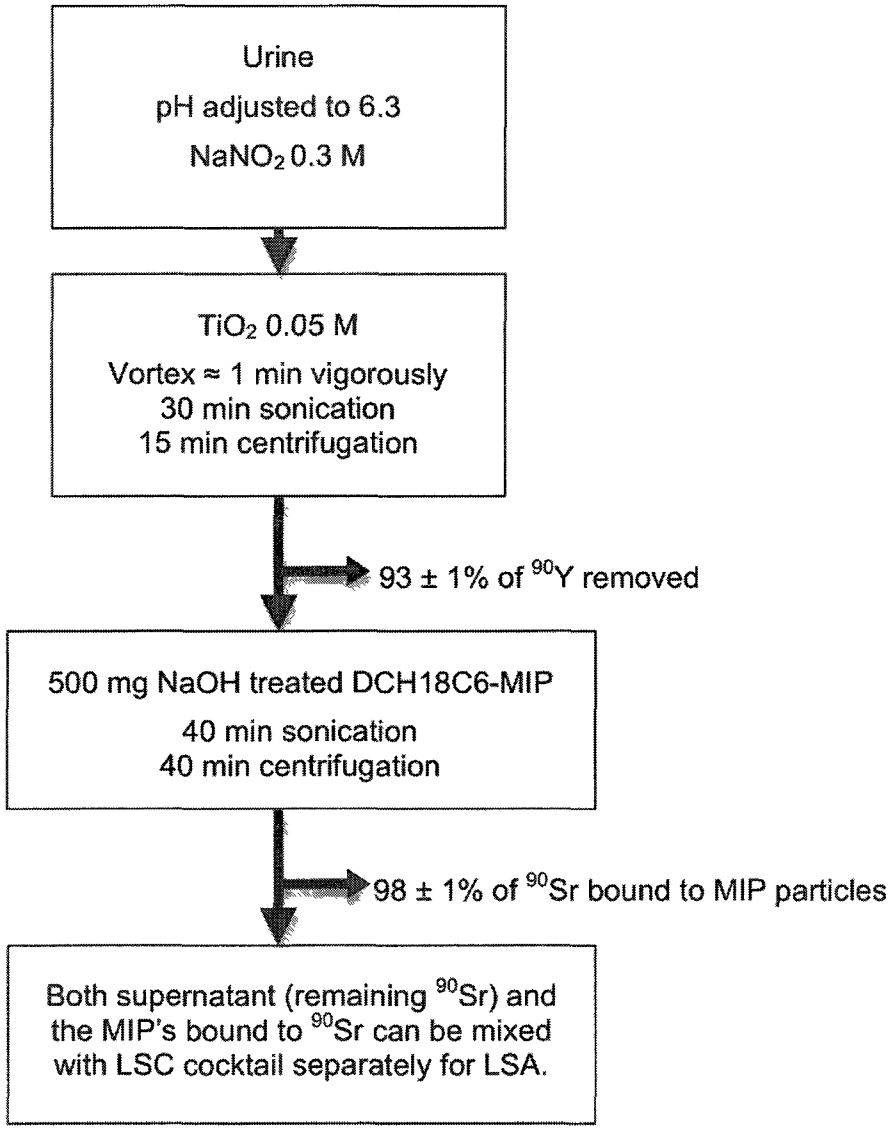

Scheme 3 Flow diagram on sample preparation and analysis of 100 Bq $^{90}Sr/^{90}Y$ in 3 mL urine. ^{90}Y was removed by TiO_2 (0.05 M, or 0.012 g dry TiO_2 added into 3 mL of urine sample).

CHAPTER IV

CONCLUSIONS

4.0 Conclusions

In the present work, ^{90}Sr uptake onto MIP particles (either imprinted with E2 or incorporated/impregnated with DCH18C6) was investigated. DPASV, AES, gamma spectroscopy and LSC have been successfully used to characterize their metal ion binding properties, in hopes for robust SPE of Sr^{2+} in urine samples. DCH18C6-MIP particles were successfully prepared (and characterized) for binding with strontium in urine samples. After NaOH treatment, the particles attained a 98±1% binding of Sr^{2+}. Interference from ^{90}Y was minimized by TiO_2 addition, followed by centrifugation that removed as much as of 94% yttrium out of the urine sample. These NaOH-treated DCH18C6-MIP particles, once prepared in the lab, are absolutely field-deployable for population monitoring after a radiological or nuclear emergency. The high % ^{90}Sr uptake onto NaOH-treated DCH18C6-MIP particles remained constant in the ionic strength range from 0.1 to 0.5. This would be advantageous, considering that the ionic strength of urine ranges from 0.1 to 0.5 (with an average of 0.32) based on individual diets and geography populations.[70] This new analysis method is easy, cost effective and requires only a turnover time of 2 hours. Alternatively, these MIP particles can be transferred into the LSC cocktail for direct liquid scintillation analysis.

4.1 Future studies

The binding capacity of these NaOH-treated MIP particles should be further investigated, in terms of how large the urine sample volume (urine) can be. More research work can be done to optimize/maximize ^{90}Y sorption onto TiO_2. Future studies can focus on optimization and automation of the method for field-deployed urine

analysis. Automation can be made easy by adding a super-paramagnetic core inside these DCH18C6-MIP particles.

Further selectivity studies on these MIP particles are worth attempting. The uptake of other metal ions onto these NaOH-treated DCH18C6-MIP particles can be investigated for waste management and purification purposes, which would provide a viable solution to several environmental health related problems.

References

1 Environmental Emergency Response Division, CRTI projects, Environment Canada, 2006.

2 Defence Research and Development Canada http://www.css.drdc-rddc.gc.ca/crti/index-eng.asp

3 Radiation Safety Manual, Veterans Affairs Palo Alto, Health Care System, March 2010.

4 A.P. Vonderheilde, M.V. Zoriy, A.V. Izmer, C. Pickhardt, J.A. Caruso, P. Ostapczuk, R. Hille, J.S. Becker. Journal of Analytical Atomic Spectrometry. 2004, 19, 675-680.

5 A.L. Hector, W. Levason, M. Webster. Inorganica Chimica Acta. 2000, 298, 43-49.

6 M.J. O'Hara, S.R. Burge, J.W. Grate. Analytical Chemistry. 2008, 81, 1228-1237.

7 G. Pisarcikova, L. Zavodska, J. Lesny. Nova Biotechnologica. 2007, 7,1 93-100.

8 A. Plionis, G.R. Gonzales, S. Landsberger, D.S. Peterson. Applied Radiation and Isotopes 2009, 67, 14-20.

9 B. Sadi, C.S. Li, S. Jodayree, E.P.C. Lai, V. Kochermin, G. Kramer. Radiation Protection Dosimetry. 2010, 140, 41-48.

10 C.S. Li, B. Sadi, G. Moodie, J.N. Daka, E.P.C. Lai, G. Kramer. Radiation Protection Dosimetry. 2009, 136, 2, 82-86.

11 S. Brun, Y. Kergadallan, B. Boursier, J.M. Fremy, F. Janin. Dairy Science and technology, Lait, 2003, 83, 1 -15.

12 A. Molinelli, R. Weiss, B. Mizaikoff. Journal of Agricultural and Food Chemistry. 2002, 50, 1804-1808.

13 C.S. Li, D. Wilkinson, K. Yu. Public Security S&T Summer Symposium 2010 Proceedings, CRTI 06-0230RD.

14 X. Hou. Riso National laboratory for sustained energy. Technical university of Denmark. NKS-218, ISBN 978-87-7893-288-4, 2010.

15 J. Thomson. Liquid Scintillation Counting Application Notes LSC-007. Packard Bioscience, 2001.

16 National Diagnostics Laboratory Staff. Principles and Applications of Liquid Scintillation Counting. National Diagnostics. 2004 EUROPE: 441 482 646022

17 User Guidelines and Standard Operating Procedure for Beckman Coulter LSC6500. Laurier Research Instrumentation.

18 Hidex, Quench Correction and DPM calculation in Triathler, setting discrimination windows. Application note Traithler technical features. DOC 411-004

19 E.H. Borai, E.A. El-Sofany. Journal of Radioanalytical and Nuclear Chemistry. 2004, 262, 3, 697-701.

20 P.L. Kole, G. Venkatesh, J, R. Sheshala. Biomedical Chromatography. 2011, 25, 199.

21 J. S. Fritz. Analytical Solid-Phase Extraction. John Wiley & Sons Inc., NY. 1999.

22 Y. Chen, M. Kele, P. Sajonz, B. Sellergren, G. Guiochon. Anaytical Chemistry. 1999, 71, 928.

23 D. Kriz and K. Mosbach. Analytica Chimica Acta, 1995, 300, 71–75.

24 A. Opik, A. Menaker, J. Reut, V. Syritski. Proceedings of the Estonian Academy of Sciences. 2009, 58, 1,3-11.

25 C. Malitesta, R.A. Picca, G. Ciccarella, V. Sgobba, M. Brattoli. Sensors 2006, 6, 915-924.

26 M. Yan, O. Ramstrom. Molecularly Imprinted Materials Science and Technology, Marcel Dekker, NY, 2005.

27 S. Boonpangrak, M. J. Whitcombe, V. Prachayasittikul, K. Mosbach, L.Ye. Biosensors and Bioelectronics. 2006, 349-354.

28 H. Yan, K.H. Row. International Journal of Molecular Sciences. 2006, 7, 155-178.

29 J.C.C. Yu, E.P.C. Lai. Toxins. 2010, 2, 1536-1553

30 G. Subramanian. Chiral separation techniques: a practical approach. Wiley-VCH 2007.

31 A. Favre-Reguillon, N. Dumont, B. Dunjic, M. Lemaire. Tetrahedron. 1997, 53,4, 1343 – 1360

32 C. Pasel, A. Elsner. Practical Exercise Instruction, Heavy Metal Precipitation. Duisburg-Essen. 2006.

33 A. Boda, S.K. Musharaf Ali, R.K. Shenoi, H. Rao, S.K. Ghosh, Jornal of Molecular Modeling. DOI: 10.1007/s00894-010-0812-7

34 H.S. Andersson, O. Ramstro. Journal of Molecular Recognition. 1998, 11, 103 -106.

35 W.D. Ehman, D.E. Vance. Radiochemistry and Nuclear Methods of Analysis, Wiley & Sons Inc., South Carolina, 1991

36 P. Peerani, Esarda Bulletin, 2006, 35, 64-67.

37 H. Bomben, H. Equillor, A. Oliveira, Journal of Radioanalytical and Nuclear Chemistry. 1994, 177, 27.

38 A.J. Brad, L.R. Faulkner. Electrochemical Methods: Fundumentals and Aplications. John Wiley and Sons. NY 2001.

39 Skoog, Holler, Nieman. Principles of Instrumental Analysis. Saunders College Publishing. Forth Worth, TX, 1998.

40 S. Wei, A. Molinelli, B. Mizaikoff, Biosens. Bioelectron., 2006, 21, 1943–1951.

41 K. Kesenci, R. Say and A. Denizli, European Polymer Journal, 2002, 38, 1443-1448.

42 Y.M. Sun, F.Y. Dong, J.M. Dou, D.C. Li, X.K. Gao and D.Q. Wang, Journal of Inorganic and Organometallic Polymers and Materials, 2006,16, 61-67.

43 E.P.C. Lai, Z. DeMaleki and S. Wu, J. Appl. Polym. Sci., 2010, 116, 1499.

44 Z. DeMaleki, E.P.C. Lai and E. Dabek-Zlotorzynska, J. Sep. Sci., 2010, 33, 2796.

46 K. Kesenci, R. Say and A. Denizli, Eur. Polym. J., 2002, 38, 1443.

47 G.H. Rounaghi and F. Mofazzeli, Journal of Inclusion Phenomena and Macrocyclic Chemistry, 2005, 51, 205.

48 Wulfsberg G., Principles of descriptive inorganic chemistry. University Science books. Sausalito,1991.

49 C. Moreno-Castilla, M.A. Álvarez-Merino, L.M. Pastrana-Martínez, M.V. López-Ramón, Journal of Colloid Interface Science., 2010, 345, 461.

50 M.S. Tehrani, M.T. Vardini, A. Abroomand, S.W. Husain. International Journal of Electrochemical Science. 2010, 5, 88-104.

51 Y. Shu, G. Ou, L. Wang, J. Zou, Q. Li. Journal of Nanomaterials. doi:10.1155/2011/423686.

52 E. Pamula, E. Dryzek. Acta Physica Polonica A. 2008, 113, 5, 1485 – 1493.

53 M.L. Ngiam, S. Dhara, B. Su. European Cells and Materials. 2005, 10, 70.

54 M.R. Soares, J.C. Casagrande, E.R. Mouta. Communications in Soil Science and Plant Analysis. 2009, 40,13 2132-2151.

55 C.Moreno-Castilla, M.A. Alvarez-Merino, L.M, Pastrana-Martinez, M.V. Lopez-Ramon. Journal of Colloid and Interface Science, 2010, 345, 461-466

56 H. Liu, B. Qing, X. Ye, Q. Li, K. Lee, Wu. Chemical Engineering Journal. 2009, 235 – 240.

57 R.M. Harrison. Understanding our environment; an introduction to environmental chemistry. Royal Society of Chemistry. Cambridge, 1999.

58 F. Faridbod, M.R. Ganjali, R. Dinarvand, P. Norouzi, S. Riahi. Sensors. 2008, 8, 1645-1703.

59 A. Usuda A, K. Kono, S. Hayashi, T. Kawasaki, G. Mitsui, T. Shibutani, E. Dote, K. Adachi, M. Fujihara, Y. Shimbo, W. Sun, B. Lu, K. Nakasuji. Environmental Health and Preventive Medicine 2006, 11, 11-16.

60 C. Pasel, A. Elsner. Heavy Metal Precipitation. Practical Exercise Instruction. University Duisburg-Essen. 2006.

61 A.L. Hector, W Levason, M. Webster. Inorganica Chimica Acta 2000, 298, 43-49.

62 A. Isaacs, J. Daintith, M. Elizabeth, Concise Science Dictionary. Oxford University.1984

63 N.J. Renault, H.A. Martins. Journal of Radioanalytical Chemistry, 1980, 55, 2, 307-316.

64 M. Bouby, J. Lutzenkirchen, K. Dardenne, T. Preocanin, M.A. Denecke, R. Klenze, H. Geckeis. Journal of Colloid and Interface Science, 2010, 350, 551-561.

65 D.J. Wesolowski, M.L. Machesky, M.K. Ridley, D.A. Palmer, Z. Zhang, P. Fenter, M. Predota, P.T. Cummings. ECS Transactions, 2008, 11, 27 167-180.

66 X. Xie, L. Gao. Current Applied Physics. 2009, 9, S185-S188.

67 P.K. Dutta, A.K. Ray, V.K. Sharma, F.J. Millero. Journal of Colloid and Interface Science. 2004, 278, 270-275.

68 B. Fernandez-Ibanez, S. Malato, F.J. De Las Nieves. Boletin de la Sociedad Espanola Ceramica y Vidrio Articulo. 2000, 39, 4, 498-502

69 A. Georgaka, N. Spanos. Global Nest Journal, 2010, 12, 3, 239-247

70 J.S. Elliot, R.F. Sharp, L. Lewis. J. Phys. Chem. 1958, 62, 6, 686 - 689